Marcel Zube, BSc

EEG–based Neuroprosthesis

Master thesis

Biomedical Engineering

Supervisor

Gernot R. Müller-Putz, Univ.-Prof. Dipl.-Ing. Dr.techn.

Institute of Neural Engineering
Laboratory of Brain-Computer Interfaces
Graz University of Technology
Stremayrgasse 16/IV, 8010 Graz, Austria
Head: Univ.-Prof. Dipl.-Ing. Dr.techn. Gernot R. Müller-Putz

Graz, February 2019

EIDESSTATTLICHE ERKLÄRUNG

AFFIDAVIT

Ich erkläre an Eides statt, dass ich die vorliegende Arbeit selbstständig verfasst, andere als die angegebenen Quellen/Hilfsmittel nicht benutzt, und die den benutzten Quellen wörtlich und inhaltlich entnommenen Stellen als solche kenntlich gemacht habe. Das in TUGRAZonline hochgeladene Textdokument ist mit der vorliegenden Masterarbeit identisch.

I declare that I have authored this thesis independently, that I have not used other than the declared sources/resources, and that I have explicitly indicated all material which has been quoted either literally or by content from the sources used. The text document uploaded to TUGRAZonline is identical to the present master‘s thesis.

_____ _____

Datum / Date Unterschrift / Signature

Acknowledgement

In this section I would like to thank all those who contributed to the success of this master thesis by sharing their experience in the field of science. First, I want to thank my supervisor Prof. Dr. Gernot Müller-Putz, who guided me through the world of neurotechnology and gave me the opportunity, not only to write this thesis, but furthermore, expand my experience and knowledge within this field by working in the MoreGrasp project. This leads me to the next appreciation for all members of the MoreGrasp-team, especially Joana Pereira, Patrick Ofner, Matthias Schneiders, Andreas Pinegger and Carlos Escolano to support and fully integrate me from the very beginning and share their expertise with me. In particular, I would like to thank Andreas Schwarz, who introduced me to scientific work and without his extensive support this thesis would not have been possible. Finally, I want to thank all my colleagues at the Institute for Neural Engineering, my family and friends to motivate and provide assistance during the time I have been working on this thesis.

Abstract

For people with a spinal cord injury (SCI) leading to a motor impairment, one of the highest desires is to get back a part of their autonomy, which could be reached artificially by giving them back some sort of control of their body functions. A neuroprosthesis helps to do so, by electrically stimulating the right muscle groups. In this case, it stimulates the muscles of the upper extremities to restore grasp functions. There are a lot of possibilities to control such a neuroprosthesis, like electroencephalography (EEG), electromyography (EMG), motion sensors and many more. This thesis provides a modular workspace to control a functional electrical stimulation (FES) device, especially with EEG and a shoulder position sensor, where it is easy to add more control elements. The implemented wireless communication with the stimulation device is constructed in MATLAB and can be adapted to any type of control elements. Within a study, the assembled parts are evaluated and improved. Evaluation has shown that the shoulder position sensor works for healthy as well as for tetraplegic people and can be used in any environment of daily living. Anyway, it has the big disadvantage of being counterintuitively. Because of this, a quite new way, where a lot of research is ongoing, offers the basis for the EEG-control modality. A study investigates the neuroprosthesis control via low frequency time domain signals from the primary motor cortex (movement-related cortical potentials) measured via a wireless water-based EEG system. Results show an online accuracy up to 70 percent for movement versus movement classification. The average over all participants is still low (about 62 %) and a lot of research has to be done to improve this type of control.

As a conclusion, it can be said that with some additional modifications the system provides a highly promising solution to improve daily life quality for people with spinal cord injury.

Key words: Neuroprosthesis, EEG, functional electrical stimulation, movement-related cortical potential, spinal cord injury

Zusammenfassung

Der größte Wunsch für Personen mit Tetraplegie ist es, einen Teil ihrer Selbständigkeit wieder zu erlangen. Dieses Ziel kann, unter anderem, durch Neuroprothesen erreicht werden, welche bestimmte Muskelgruppen mit elektrischen Impulsen stimulieren und damit die noch innervierten Muskeln anregen. In dieser Arbeit werden speziell die Muskeln der oberen Extremität behandelt, um verschiedene Arten des Greifens künstlich wiederherzustellen. Neben der Anregung der Muskelgruppen ist auch die Steuerung dieser Neuroprothese Teilgebiet der Arbeit. Deshalb wurde eine Umgebung implementiert, welche das Stimulationsgerät via Elektroenzephalografie (EEG) und mit einem Schulter-Positions-Sensor steuern kann. Die Realisierung in MATLAB ist modular aufgebaut, um eine Erweiterung oder Änderung auf andere Steuerungen einfach zu ermöglichen. Jene zwei Arten der Steuerung wurden jeweils im Zuge einer Studie evaluiert. Der Schulter-Positions-Sensor ermöglicht Personen mit Tetraplegie den Einsatz der Neuroprothese für spezifische Tätigkeiten im Alltag. Er hat jedoch den Nachteil nicht intuitiv zu sein. Die Steuerung mittels EEG, welche niedrig-frequente Signale im Zeitbereich (movement-related cortical potentials) innerhalb eines cue-basierten Paradigmas benutzt, erreicht online bei der Klassifikation zweier Bewegungen eine Genauigkeit von maximal 70 %. Jedoch liegt der Durchschnitt aller Probanden nur bei 62 % und um das Potential dieser Steuerung auszuschöpfen sind weitere Modifikationen notwendig.

Zusammenfassend stellt das implementierte System eine Basis für weitere zukünftige Studien dar, um eine verbesserte Lebensqualität für Personen mit Rückenmarksverletzungen zu gewährleisten.

Schlüsselwörter: Neuroprothese, EEG, funktionelle elektrische Stimulation, kortikale Potentiale durch Bewegungen, Rückenmarksverletzung

Contents

Abbreviations

AP	Action Potential
ASIA	American Spinal Injury Association
AIS	ASIA Impairment Scale
BBT	BitBrain Technologies
BCI	Brain-Computer-Interface
CAR	Common average reference
CU	Computational Unit
ECoG	Electrocorticography
EEG	Electroencephalogram
FES	Functional electrical stimulation
FESMUX	Stimulation Device of the MoreGrasp Project
FPR	False positive rate
GUI	Graphical User Interface
MRCP	Movement-related cortical potential
SCI	Spinal cord injury / spinal cord injured
(s)LDA	(Shrinkage) linear discriminant analysis
TPR	True positive rate

1. Introduction

This introduction gives an overview of anatomical and physiological structures in the context of spinal cord injury (SCI) based on [1] and [2] and also highlights the motivational background behind this thesis

1.1 Anatomical, physiological and technological Background

An SCI means a major change in a person's life because the partial loss of independence associated with it represents a challenge not only for a person himself but also for one's family and friends. Depending on the level of injury it is possible that the affected person even loses the ability to perform simple activities of daily living (ADL) like grasping a glass of water or hygienic necessities. Lesions above a certain level lead to disturbed function of upper extremities. One of the greatest desires for people with cervical SCI is the improvement of hand and arm function to get back a certain degree of independence. [3] [4]

1.1.1 Central Nervous System - Spinal Cord

The nervous system is built up from a network of connected neurons which communicate with each other. A neuron consists of a cell body, so called soma, axon and the dendrites. The dendrites work as an interface to other nerve cells while the axon is the transmitting unit of a neuron. Neurons communicate with other cells by action potentials (AP). An AP is generated if the axon experiences a depolarization which exceeds a specific threshold of excitation. [5]

As a part of the central nervous system the spinal cord is, among many more functions, responsible to exchange information with the brain for voluntary control of muscles. It is segmented in eight cervical, twelve thoracic, five lumbar, five sacral and one coccygeal parts, defined by the origination of the spinal nerves.

Spinal Cord Injury

If a vertebral fracture or dislocation occurs, local damage to the spinal cord, caused by axonal rupture or compression, emerges (primary damage). As a direct consequence, the surrounding tissue gets harmed due to ischemia, bleeding and edema (secondary damage). Some additional factors, which contribute to the structural and functional damage, are inflammatory reactions or the death of neurons and glia cells.

Such fractures can lead to paralysis, caused by an interruption of the efferent and afferent nerve pathways. Depending on the extent of the injury the paralysis could be a complete

paralysis, which leads to a full loss of function below the injured segment, or, if there is a sign for some remaining functionality, the paralysis is stated as incomplete. Another differentiation can be made due to the level of injury. If the level of injury is above C8, it is called tetraplegia (also called quadriplegia) and below this region it is called paraplegia. In Figure 1 the affected areas and functions depending on the level of injury are shown. [6]

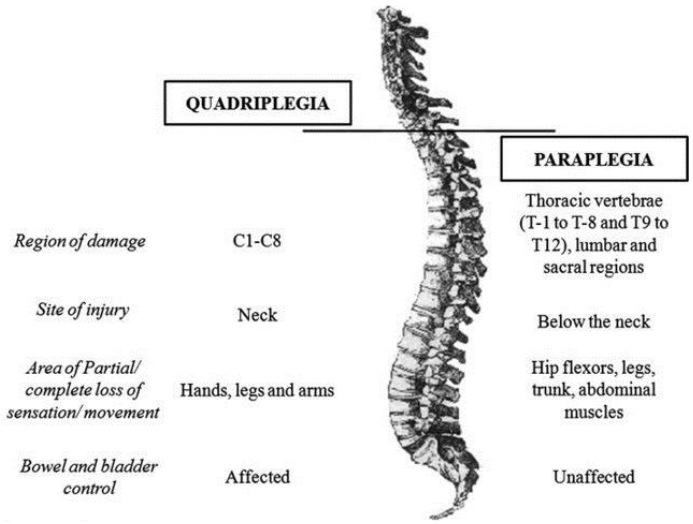

Figure 1: Tetraplegia and Paraplegia, affected areas and functions [6]

Spinal Cord Injury - Treatments

Even though there are several approaches to restore the spinal cord itself at the neurobiological level based on neuroprotection, neurorestoration and neuroregenerative therapies, the solution of this problems is still far in the future. [7]

Another possibility to improve the functions of the upper extremity is surgical treatment. Depending on the patient, muscles with suitable residual function, so called donor muscles, are used to maximize hand and arm functions with the help of invasive surgery. For example, arthrodesis is used to increase the muscle efficiency by minimizing the number of joints a muscle is attached to and creating a good position to ensure the intended grasp. There are several more surgical procedures which can be used, but all of them have in common that donor muscles are needed to create the desired functionality. This requirement is not given for high SCI above C5 and therefore, the function can be restored with some sort of neuroprosthesis based on electrical stimulation. [8]

1.1.2 Neuroprosthetics

In the field of neuroprosthetics, motoric, sensory or vegetative nerve functions are supported or restored by artificial electrical stimulation [9]. They are used for several different clinical applications like the cardiac pacemaker, which restores functions of the cardiac electrical conduction system via functional electrical stimulation (FES) and is the first implanted FES-device in history. Another application is the cochlear implant, where the Nervus Accusticus is stimulated to restore auditory function. Other applications are the stimulation of sacral nerves to prevent incontinence or the control of respiration by stimulating the Nervus Phrenicus. The general structure or operating principle usually stays the same for all neuroprosthesis. Sensor systems capture a control signal which is preprocessed and then used for the stimulation. [10]

Functional Electrical Stimulation

In this thesis, the focus lies on the functional restoration of the upper extremities based on FES. The muscle contraction should be controlled via external electrical impulses instead of the common transmission from the brain through the spinal cord and peripheral nerves to the muscle. Muscles of the human body are differentiated in three types due to physiological properties. First, the smooth muscles, which occur in the walls of the hollow organs, except the heart, cannot be controlled voluntarily. The second muscle group is the cardiac muscle. It is responsible for the contraction of the heart. Third, the muscle group that is the most important one for the investigated research question, is the skeletal muscle. This group is needed for the voluntary movements of the human body. Such skeletal muscles are structured into three different types of muscle fibers. The fiber types differ for example in the speed of contraction or the force produced. By activating each of the different muscle fiber types to a certain degree a movement can be performed [11]. Each muscle fiber is connected to one motoneuron, but every motoneuron innervates a variable number of muscle fibers, depending on the size and excitability of this motoneuron. One single motoneuron and its associated muscle fibers form a motor unit. The motor unit might be seen as the functional unit of the muscle [12] [13]. Some properties of the fiber types and the corresponding motor units are listed in Table 1.

Table 1: Characteristically differences of muscle fiber types, edited from [14]

Characteristics	Fiber Types		
	Type 1	Type 2A	Type 2B
Physiological Function	Sustained forces	Powerful, phasic movements	
Motoneurone firing threshold	Low	Intermediate	High
Motor unit size	Small	Large	Large
Maximum shortening velocity	Slow	Fast	Fast
Rate of relaxation	Slow	Fast	Fast
Resistance to fatigue	Resistant	Intermediate	High
Excitability to external trigger	Low	Intermediate	high

In case of a neuroprosthesis, artificially controlled electrical impulses depolarize an intact motoneuron to trigger an AP. The generated AP spread out to the motor units and lead to a contraction of the muscles. Nerve fibers and muscle fibers are responsive to external applied electrical current, for FES usually a direct stimulation of the nerve fibers is done since lower electrical currents are needed to get an AP. The transmission of the electrical impulses is carried out by pairs of electrodes. In general, there are different types of electrodes which can be used for the stimulation. Percutaneous (placed under the skin) and fully implantable epimysial electrodes are invasive methods and not further explained and used within this thesis. A non-invasive approach is the usage of surface electrodes [15]. To give an overview of the behavior when using surface electrodes for stimulation it is referred to [16].

Stimulation Parameter

By using a rectangular wave form for the stimulation, two values must be considered to elicit an AP, the amplitude and the time of the stimulation pulse. This means that a depolarization of the excitable membrane is dependent on the transferred charge through the membrane and can be calculated by equation (1). To describe the effect of electrical stimulation for different tissues, two parameters are defined. First, the rheobase is defined as the amplitude of the current needed to trigger muscle activation at an infinite impulse length. Second, the chronaxie specifies the minimum duration of the applied stimulation pulse to cause an excitation at an amplitude value twice the rheobase. In equation (2), the lapicque equation, the dependencies between these values are described and with this equation it is possible to calculate the minimum amplitude to trigger a motoric reaction at defined pulse duration [17]. Sensory fibres show a lower rheobase than motoric fibres, which means before motoric

reaction starts, a sensory feedback occurs [18]. Detailed descriptions of stimulation behavior can be found in basic literature [19].

$$Q = I * t \tag{1}$$

Q	Charge in As
I	Current amplitude in A
t	Duration of the impulse in s

$$I = b * (1 + \frac{c}{t}) \tag{2}$$

I	Current amplitude in A
t	Duration of the impulse in s
b	Rheobase in A
c	Chronaxie in s

Most stimulation devices use a biphasic stimulation pattern and three parameters, the frequency, the amplitude and the pulse width, to control the output. To control the force of a specific muscle group, it is necessary to understand the effect of changing these parameters. Artificial stimulation, other than physiological activation, activates larger motor units earlier and therefore, it is important to care about the muscle fatigue when specifying the parameters. In case of the frequency, a tradeoff between muscle fatigue and smooth contraction has to be found. Usually, the frequency is above 15 Hz to avoid twitching of the muscles. The amount of activated motor units could be increased by changing the pulse amplitude or duration to increase the electrical charge. [20]

To summarize, a neuroprosthesis for the upper extremities work with defined inputs from several sources to control predefined grasp or movement pattern. In general, it is possible to design such a system as open- or closed loop system. For a closed loop system, some sort of feedback is necessary. Examples for feedback are the force produced [21] or feedback processing via EMG-signals [22]. Moreover, open loop systems have the advantage of a simpler design and less necessary hardware. Literature has shown that already an open loop control can be efficiently used for a neuroprosthesis [23].

1.1.3 Brain Computer Interface

Furthermore, a possible source to control such a neuroprosthesis could be the brain itself. For healthy persons a series of APs, usually originate in the brain, lead to muscle activation, whereas for SCI this pathway is interrupted. Therefore, it is necessary to measure and further process the signals that come from the activity of the brain to bypass the injured region and build a so-called Brain-Computer-Interface (BCI) [24] [25].

As even simple movements, like reach and grasp movements, are quite complex motor tasks, many brain regions are involved when executing these tasks. The whole motor system of the human body is structured hierarchically, whereas the motor and premotor cortices are on top of this hierarchy, mostly responsible for less automatic motor control. In Figure 2 the location of brain areas for motor control are visualized. If a movement is planned, one of the main areas involved in this planning phase is the premotor cortical region. The motor cortex is responsible to control the movement execution and forward all the necessary motor commands to finally control a set of muscles. Control signals and resulting sensory signals are analyzed by the cerebellum, which is responsible for the precise coordination and timing of the movement [26]. Within the motor cortex, every part of the body could be represented at a different location and in a different extent. For parts of the body where more complex control is necessary, for example the hand, the regions are larger and, the other way around, for body parts where only a limited movement complexity is given, the representative areas on the motor cortex are smaller. Another interesting fact is that signals from the motor cortex are crossed and commands for the left side of the body are represented on the right hemisphere and vice versa. [27]

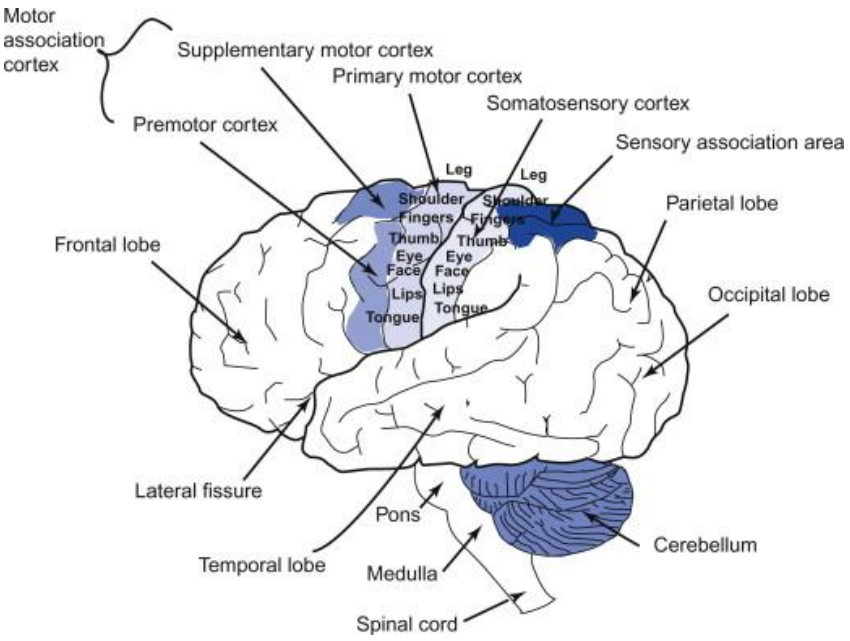

Figure 2: left - Division of brain areas responsible for motor control; Modified from [27]

Brain activity can be measured invasive and non-invasive. Concentrating on the portable systems, most used methods are the non-invasive electroencephalography (EEG) and the invasive electrocorticography (ECoG). Because surgery always entails risks, EEG is preferred for most BCIs. Also, non-invasive optical imaging (fNIRS) is portable, but its measurement principle relies on metabolic processes and compared with EEG and ECoG it offers a low temporal resolution. EEG provides good temporal resolution without the need of high-cost and big devices. The electrical activity of the brain is measured with a defined number of electrodes distributed and placed over the scalp depending on the signal to investigate [28]. Even though, the distance to the origin of the specific signal is quite high and only reduced amplitude and a limited spatial resolution can be achieved. Moreover, the EEG has shown to be a sophisticated solution for BCIs [29]. The typical structure of such a BCI is shown in Figure 3.

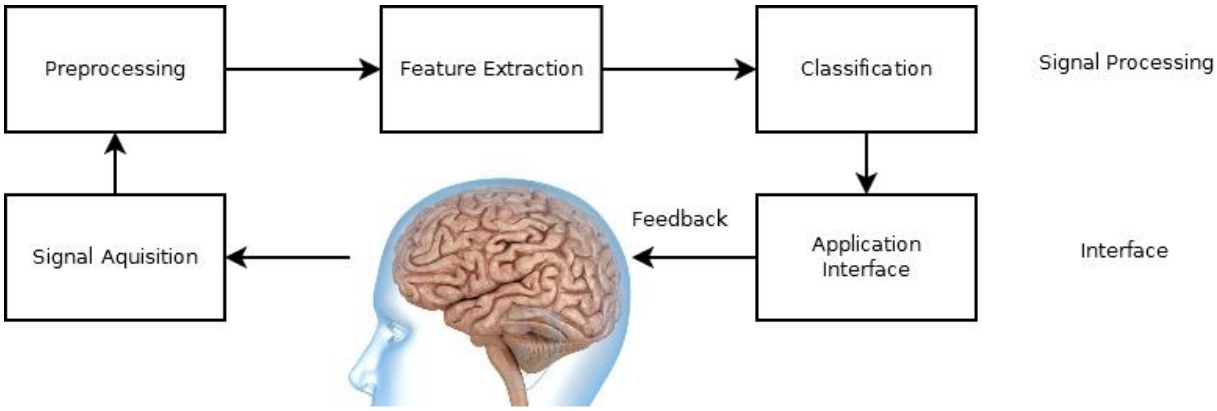

Figure 3: Typical process pipeline for a BCI

Movement-related cortical potentials

The possibility to control a device with an EEG-based BCI has already been researched for quite a long time [30] [31]. However, most of these studies focused on signals that are quite well distinguishable in the generated EEG-signal, but do not provide a truly intuitive, realistic situation for the user. For example, repetitive movement of both feet are used to control upper limb functionalities or the lateralization of movements was exploited to distinguish between brain signals and process commands aimed to control one hand [32] [33]. A new sophisticated way to get a more intuitive type of control is to decode the movement attempt/execution of a single movement that is directly related to the executed movement of the neuroprosthesis. For example, when an end-user wants to grasp a glass with the neuroprosthesis, he should try to execute, in this case, the palmar grasp and the BCI System recognize his attempt and further process the command to the neuroprosthesis. Already promising results were shown with invasive ECoG [34]. When looking at the time domain signal in the low frequency range (below 6 Hz) during a movement execution/attempt, activation at the motor cortex lead to a signal called movement-related cortical potential (MRCP). While the participant is preparing for a movement, a negative amplitude shift can be observed, leading to a maximum negativity at the time of the movement onset. After this negativity the wave usually has a positive overshoot and returns to its resting level. This signal has a high variability and its waveform is influenced by a lot of factors like the intention, pace, effort, force, speed, complexity and precision of the movement [35]. Research, according classification of this low frequency time domain signals with EEG, already were able to process significant differences in the signals of hand movements leading to the result that a classification should be possible for non-invasive methods [36] [37].

1.2 Motivation and Aim

At the Graz University of Technology, Institute of neural engineering, there is already a neuroprosthesis system with several input modalities like EEG, shoulder position sensor and instrumented objects tested and in use by end-users. It was built within the MoreGrasp Project[1]. The MoreGrasp System is a highly specialized and complex system including a lot of different programming languages and especially a lot of expensive soft- and hardware is needed to run it. Because of this, the need to implement an additional, simpler system or environment, which can be used and adapted easily for different research questions and teaching to directly reduce the threshold of using a neuroprosthesis within those areas arose. The outcome of this thesis is a neuroprosthesis, implemented in a development environment that is tested already for 2 input sources, the shoulder position sensor and the EEG. EEG-control is evaluated and analyzed within a study to collect data, gain knowledge and detect improvements on intuitive EEG-based control.

Next, the characteristic features of the Implementation are listed:

Simplicity

At least, components of the environment must be usable for several different tasks, so it is necessary to keep the software and the hardware architecture as simple as possible.

Mobility

Part of the concept is the possibility to use elements of the implementation for research in the laboratory as well as for end-users at their homes. For practical reasons, the environment should work with mobile components that means with lightweight and in best case wireless devices.

Modularity

One of the most important aspect is the modularity. It is essential to build the control possibilities of the neuroprosthesis adaptable to ease adding new features and new control methods.

[1] www.moregrasp.eu

Usability

Of course, for people with engineering background, a base level of technical understanding can be assumed, but for end-users, which includes people with SCI or other disabilities, this prerequisite should not be mandatory to use the neuroprosthesis. Because of this, it should be possible for end-users to use at least some components of the realization after an appropriate instruction from an expert, even if, in the background, the complexity stays high.

Out of these properties, following requirements were defined:

- Implementation as a MATLAB/Simulink (MathWorks Inc) model
- Control of the neuroprosthesis via shoulder position sensor and EEG
- Wireless communication between the computational unit (CU) and neuroprosthesis components (EEG, FES-device)
- Additional possibility to use a standard wired FES-device
- Evaluation of EEG-control by performing a study with 10 healthy and 1 tetraplegic participants

2. Methods

2.1 Concept Design

The implemented system is designed as an open loop system so there is no feedback about the grasp performance and/or current state implemented. This is done because the benefit of adding such a device will not be higher than the additional increase of complexity, mobility and usability. Evaluation of different stimulation patterns by inspection of the grasp already led to an acceptable performance. The overview of the concept design with three implemented control methods is shown in Figure 4. The first option is a simple control via predefined keyboard inputs. As it is described in the introduction, the control via shoulder position and brain activity were also implemented. The shoulder movement is measured with a device which can be attached to the shoulder of the user and recognize the motion of the shoulder in the three-dimensional space. Brain activity is measured by a wireless EEG system. The input signals were sent to the CU and further processed to decode the correct commands. For example, the EEG processing is done with some sort of pattern recognition methods. The interface between the sensors and the CU, or more precise the FES-communication, allows to add additional sensors. After processing, the signals are converted and sent to one of the specified FES-devices to generate a grasp by electrical stimulation.

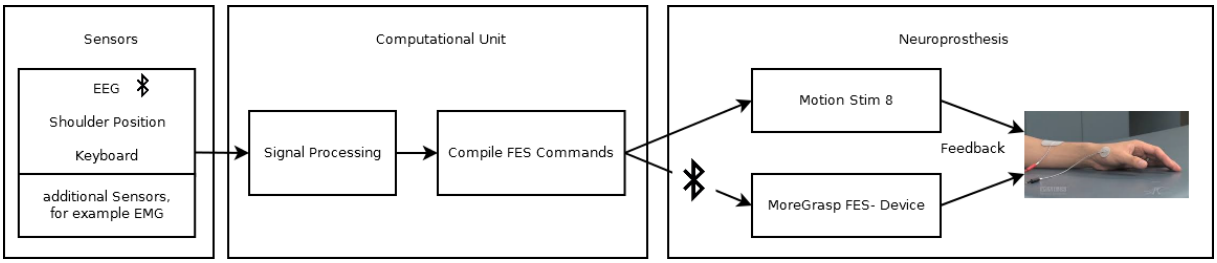

Figure 4: Conceptual structure of the neuroprosthesis control

2.2 System Setup

To meet the requirements following hard- and software was used.

2.2.1 Hardware

Computational Unit

- Lenovo ThinkPad X1 Carbon
  Windows 10 Pro (Version 1803), Intel Core i7 7500 – 2.7GHz, RAM: 16GB.

EEG Hardware

- Cap: 32-channel water-based EEG headset prototype with sintered electrodes (BitBrain Technologies (BBT))
- Amplifier: 32-channel wireless amplifier prototype (BBT)

FES-Hardware

- Option 1: MotionStim 8 (MEDEL GmbH), Connection to CU: serial connection via an optocoupling device (Krauth + Timmermann GmbH) and USB-to-serial Converter (Rotronic AG)
- Option 2: MoreGrasp FES-device prototype based on MotionStim 8 (MEDEL GmbH) with or without multiplexer
  Additional features: wireless Bluetooth connection, multiplexer for electrode arrays, microcontroller board for shoulder position sensor readout and electrode array processing
- Electrodes: hydrogel surface electrodes (Krauth + Timmermann GmbH)

Other Hardware

- Shoulder-position sensor (MEDEL GmbH)

In Figure 5 all used system components are shown. In principle, the system is a reduced version of the MoreGrasp System. As stated, it is additionally possible to use the MotionStim 8 as FES-device and a slimmed version of the MoreGrasp FES-device (without Multiplexer).

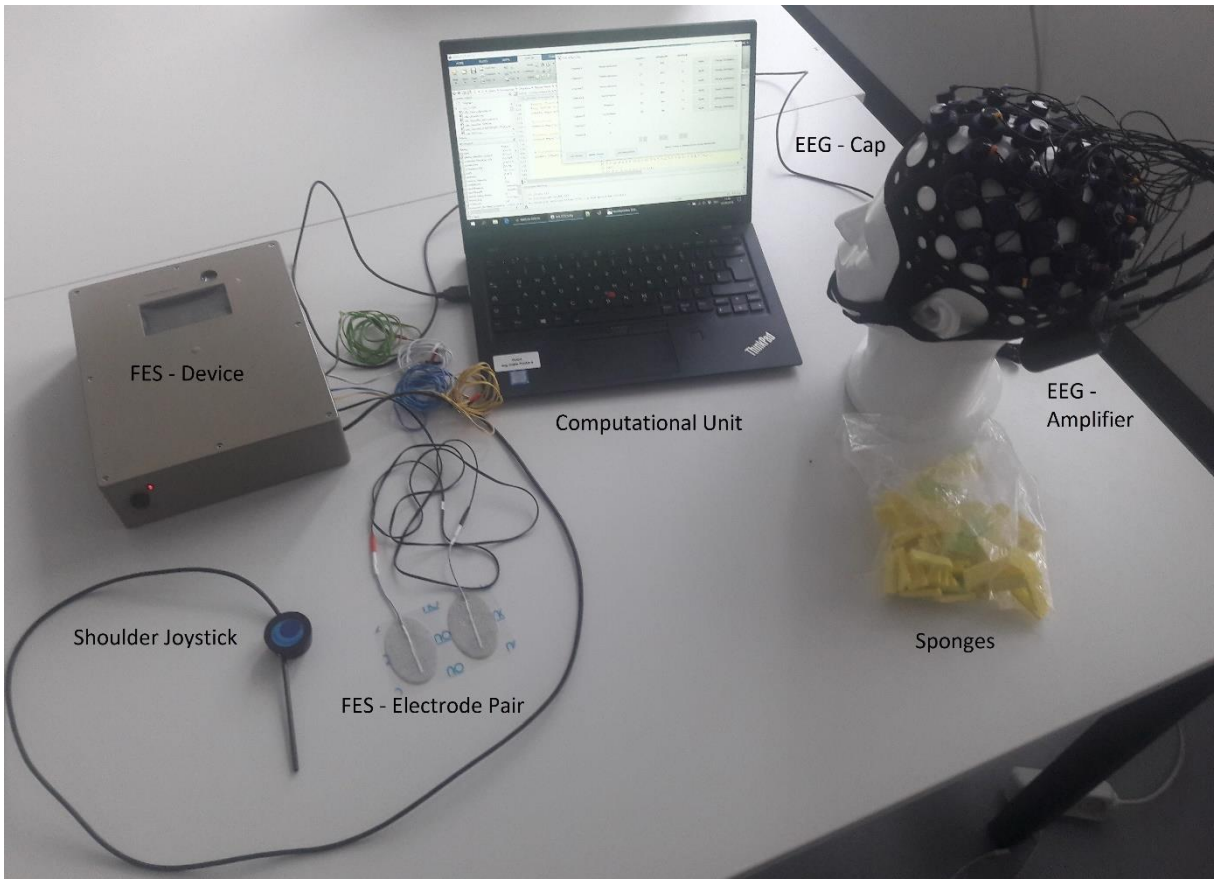

Figure 5: Applied System Components for the Neuroprosthesis

2.2.2 Software

The data processing was done in MATLAB/Simulink R2017a 64 bit (MathWorks Inc) with the advantage that only one programming language is used, which reduces the complexity, improves the usability and simplify further improvement or necessary changes.

2.3 FES – Neuroprosthesis

For a FES-system, electrical stimulation is used to restore some specific motor functions. Usually, a FES-device consists of the stimulation unit and the electrodes. Due to the concept it was clear that only one option could be considered for the type of electrodes, namely the non-invasive surface electrodes. In detail, self-adhesive hydrogel electrodes are attached to the skin to induce the specified electrical pulse.

The communication with the FES-device itself is done object-oriented. A big advantage of this approach is the given modularity. Objects are interchangeable and therefore, to add more FES-devices, only an object with the specified properties is needed to incorporate it into the given structure. For the stimulation device of the MoreGrasp project, hereinafter referred as FESMUX, such an object-oriented module already existed and it was used as a template for this thesis. Of course, some modifications were done to allow the integration into the implemented MATLAB Simulink model. Because both, the FESMUX as well as the Motion Stim 8 alone, were updated to the latest firmware that was implemented in the MoreGrasp project, parts of this template were also used for the object which handles the communication between the MS8 and the CU. The firmware allows a fast communication between the devices and the CU.

Literature has shown that the best way to manage regularized muscle stimulation is to fix the frequency and change the values of the pulse amplitude and/or pulse width [20]. A good grasp pattern could be reached by varying the pulse width values and fix the amplitude values for one movement [38].

For the first screening a configuration script with a graphical user interface (GUI) (Figure 6) is provided to save all the necessary parameters of an user as a ".mat" file into a specific folder structure. It handles the communication with both stimulation devices and simplifies the first screening of muscle stimulation parameters. Additionally, the design of the GUI avoids unwanted high stimulation values. Every channel can be labeled and each value can be defined and tested individually for all screened muscle groups. The channel number itself

states the output channel of the stimulation device. The name represents the stimulated area.

Figure 6: GUI for the parameters of the stimulation

Beside the stimulation parameter, the online system needs a map for every grasp. This map can be created with functions called create_map() and create_3Dmap() and includes information about the relation of the output pulse width to the defined movement position. For example, they show the pulse widths needed to reach the hand open position. Default grasp maps are provided for the pronation, the palmar grasp and the lateral grasp as well as for the full analog mode (explanation later) to get a palmar/pronation grasp. A map is created by defining edge parameters of the output pulse width and linearly interpolates it for the points in between. For further explanation, the usage of the map functions and the configuration file a step-by-step guide to configure the system is given in the appendix.

To obtain a module, which can also be reused and optimized in other projects, the implementation of the FES module is done as a level 2 MATLAB S-function Simulink block with several inputs and outputs. Since many adjustments for the processing of the incoming data and the communication of the FES device with the CU were made during the development process of this System, it was an ongoing process to find the most adaptive approach. A scheme of the implementation of the Simulink-block is shown in Figure 7.

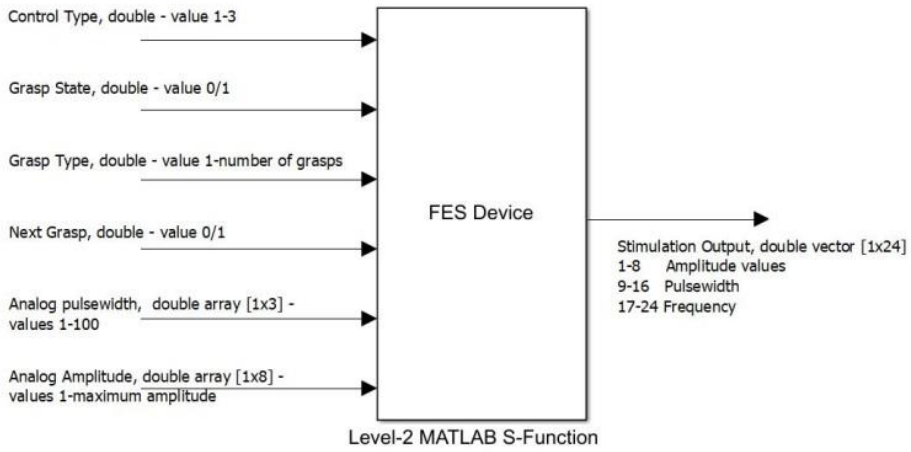

Figure 7: Schematic of the Simulink FES-block

The first input describes the control type of the neuroprosthesis. Three different control types are implemented, (1) the full digital control, (2) mixed analog/digital control, (3) full analog control. Full digital control means that even the grasp state (e.g. hand open/close) as well as the grasp type (e.g. palmar or rotation) are controlled via digital input commands. In the mixed control mode, the grasp type is controlled with digital commands and the grasp state with an analog signal in the range from 0% to 100%, depending on the configuration (grasp map) (e.g. for hand open and close: 0% →fully closed and 100% →fully open). The full analog control uses the 3D map created within the configuration and steers the stimulation output depending on the current analog input. Again, the inputs have to be converted to a range from 0 to 100. The second input of the FES-block changes the grasp state for full digital control. If this input is not zero, the grasp state changes according to its specified map from 0 (e.g. close) to 100 (e.g. open). With the third input, it is possible to change to a specific grasp and the fourth input allows to simply change to the next grasp according to the number of configured maps. Input 2, 3 and 4 are linked to each other in time and execution, which means it is not possible to execute two commands at once and also a modifiable refractory period for these commands is implemented. The last 2 inputs are analog, whereas input 5 could handle up to 3 independent control values for the pulse width regulation and input 6 was added to manually control the amplitude values of each channel. The output of the FES-block represents the current stimulation values from the device (parameter x channel). The block was tested with a maximum sampling frequency of 16 Hz whereas the limited factor is the readout process, especially of the shoulder position data.

As not only the coding, but also finding a good default grasp pattern for each required movement was part of the work, a short description of this procedure is given. To start, the default maps were created with one participant and further on these maps were improved during the EEG-study. The approximate electrode placement was done according to the motor points of the human anatomy and experience from previous experiments and experts. Stimulated muscles and their functions are shown in Table 2 [39]. Of course, for every individual, a fine tuning of the positions was needed, because the human anatomy differs from person to person. For each movement, start and endpoint were evaluated and necessary points in between were included to get a movement which is as smooth as possible and close to a physiological hand movement. To simplify the process, only agonist muscles for each movement were considered.

Table 2: Stimulated muscles and their functions

Muscle	Nerve	Origin	function	Usage
M. flexor digitorum superficialis	N. medianus	C7 – Th1	Flexion finger (2-5)	Palmar / lateral
M. abductor pollicis brevis	N. medianus	C8 – Th1	Abduction thumb	Thumb abduction
M. extensor digitorum	N. radialis	C7 – C8	Extension finger (2-5) and wrist extension	Hand open
M. extensor pollicis longus	N.radialis	C7-C8	Wrist and thumb extension	Thumb extension / hand open
M. pronator teres	N.medianus	C6-C7	Pronation and elbow flexion	Pronation
M. brachioradialis	N.radialis	C5-C7	Flexion elbow/back rotation from pronation and supination	Back rotation

The grasp performances were evaluated in terms of usability in a real life scenario. This means, for each grasp a specific usage was tested. By managing to fulfil these scenarios, the grasp was defined as realizable. Following scenarios were performed:

Palmar grasp ➔ hold a cylindrical object (height: 9 cm, Ø: 5.5 cm)

Hand open ➔ release the cylindrical object

Pronation ➔ Ability to rotate the arm 90°

Back-rotation ➔ rotate back to initial position

2.4 Alternative Control Methods

2.4.1 Keyboard

Keyboard inputs offer a simple way to control the neuroprosthesis. A level 2 MATLAB s-Function[2] converts the external keyboard input for Simulink. As the FES Simulink block can handle different types of inputs, it was only necessary to convert the keyboard inputs into the specific grasp codes. Additionally, a manual analog Simulink dashboard can simulate the input of an analog input device like a joystick, a gamepad or something similar. A detailed view of the Keyboard Simulink block is listed in the appendix.

2.4.2 Shoulder Position Sensor

The shoulder position sensor (MEDEL GmbH) is built up as two parts. One part can be connected via a MINI-DIN- port (7 poles) to the preprocessing device, in our case the Motion Stim 8 or the FESMUX, and is attached to the skin medial under the clavicula. It contains the 2-axis sensor and a button. The second part is placed more lateral on the shoulder. These specific points allow the sensor to get the position from the shoulder as a 2-axis information. Placement of the sensor parts is shown in Figure 8.

Figure 8: Placement of the shoulder position sensor

For the shoulder position sensor control a GUI, which is shown in Figure 9, offer a fast configuration process for the shoulder position sensor to save the current movement range values of the participant. The user moves the shoulder to the specified point and confirms it.

[2] By Emanuele Ruffaldi, https://www.mathworks.com/matlabcentral/fileexchange/24216-simulink-keyboard-input-v2?s_tid=prof_contriblnk

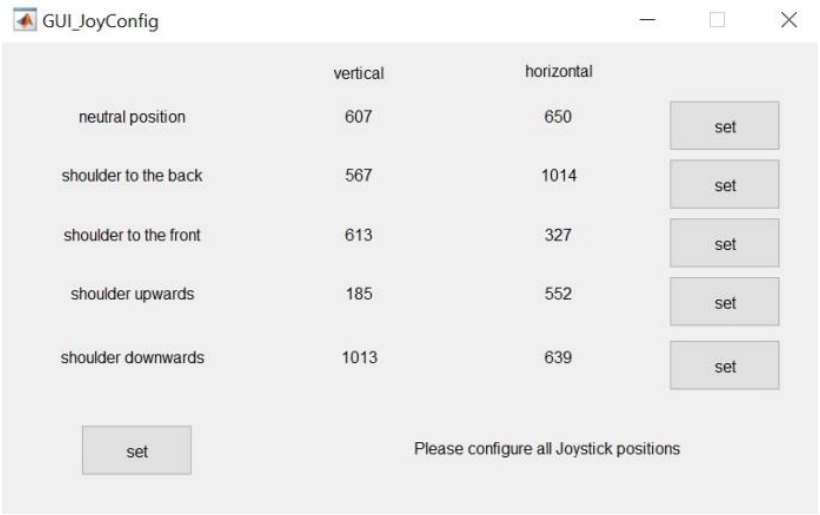

Figure 9: GUI for the shoulder position sensor configuration

To get a high performance, even for user with a small movement range and distorted movement directions, variable areas for movement detection are used. After the configuration four fixed edge points are calculated from the range of motion of the user and eight points, which can be variably defined in the configuration file, serve as borders. When starting the FES control, a field of maximum motion is created. A Matlab figure shows this maximum range of motion including the configured borders and the current location of the shoulder to provide visual feedback for the user. If a movement is out of range, it is projected to the nearest point in x and y direction inside the range of motion. With this configuration, it is easy to adapt the variable edges to the specific user movements by analyzing the movements online. The visual online feedback is shown in Figure 10.

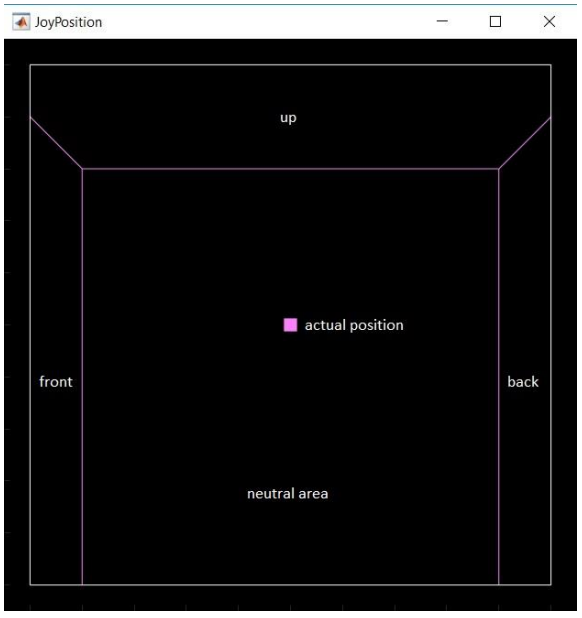

Figure 10: Areas of the shoulder position sensor processing – default configuration

Online control is handled by the Simulink process structure shown in Figure 11, whereas the sJoy_block handles the processing needed to convert the sensor values into suitable values and the s_joyvisualize_block is responsible for the visualization of the current shoulder position.

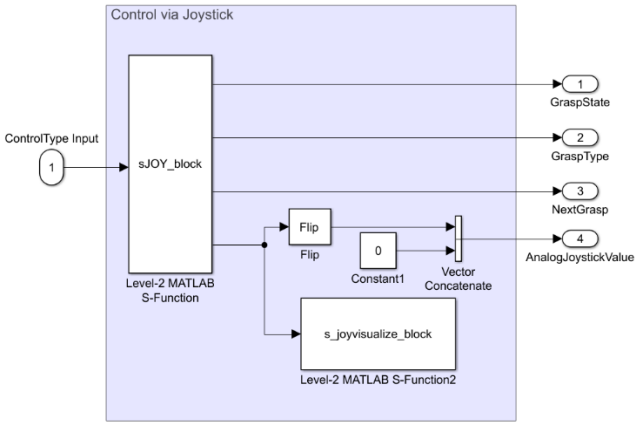

Figure 11: Simulink process for shoulder position sensor control

An evaluation of the shoulder position sensor was done with five healthy users as well as with one tetraplegic user. First, the configuration of the range of motion and the individual edge points were performed. The areas were optimized for three out of four possible movements (up, down, front, back) because the neuroprosthesis implementation allows up to three digital commands. Within the evaluation the participants were instructed to perform the movements and the output of the system was analyzed. The evaluation procedure was executed with and without the position visualized online on the screen.

2.5 EEG–based Control

Since the control of the neuroprosthesis via a BCI is a main task, the EEG-based control is written as a separate chapter, even though it is also one possibility to control the neuroprosthesis, like the keyboard and the shoulder position sensor.

2.5.1 Paradigm and experimental Setup

As it was already mentioned, for the EEG–based control a natural attempt/execution of the task should be made to control the neuroprosthesis. One possible way for classification is offered by MRCPs. To train and classify movements with MRCPs, the paradigm is one of the most important factors, because, as already described, a lot of factors influence the shape of a MRCP [35].

Participants

To test and evaluate the environment, a study with 10 healthy participants (no known medical condition) and 1 tetraplegic individual was performed. Three female and seven male persons, all right handed and between the ages of 26 to 28, took part in this study. The tetraplegic individual was 31 when participating, right handed and the level of injury is C4, sensory incomplete (B) according to the American Spinal Injury Association (ASIA) Impairment Scale (AIS). Each participant was informed about the goals and procedure of the study and an informed consent was signed beforehand. Seven out of the eleven measured persons had no previous experience in BCI experiments or EEG-measurements.

Experimental Setup

The Participants were seated in a shielded room at a distance of one meter from the screen. The hand was placed on a wide table to allow the execution of the movements. At first, the stimulation surface electrodes were placed on the right arm and the stimulation parameters were configured according to the configuration script for the palmar and lateral grasp as well as for the pronation. For the EEG-study itself only the palmar grasp and the pronation of the arm were used. Before the start of each measurement, the signal quality of the EEG signal was optimized and a test run to train the correct timing of the paradigm was executed.

The EEG was recorded with a water-based EEG-System (see 2.2.1). 32 electrodes were equally distributed over the scalp with the reference on the left earlobe. Figure 12 displays the electrode layout. EEG-recording was done with a sampling frequency of 256 Hz. The

bandwidth for the registered signal of the amplifier is from DC-40 Hz and the input range is ±100 mV.

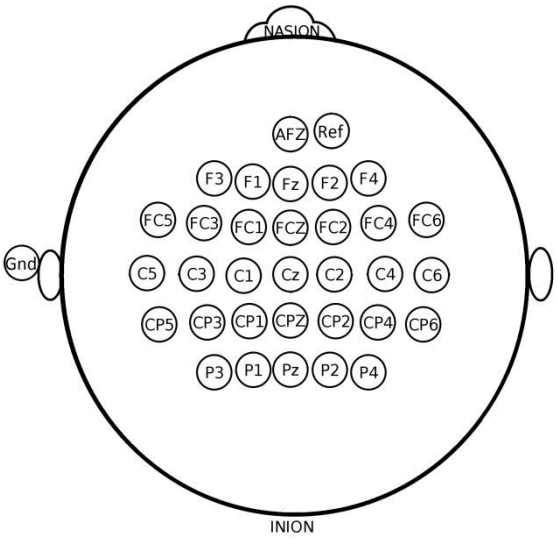

Figure 12: EEG–Cap layout, 32 channels + 1 ground and 1 reference electrode

The whole Simulink structure with FES-feedback is displayed in Figure 13. Basis for the structure is the Simulink model for measurement only and for feedback without FES, therefore these two structures are only given in detail within the appendix. A preliminary testing of the system was done to get the performance and system delay parameters as well as for testing different paradigms and their influences on the EEG-signal. The delay has been calculated for the EEG-System only as well as for the feedback system with and without the FES-device. It was measured with a signal diode to get the time difference of the cue appearance and the system.

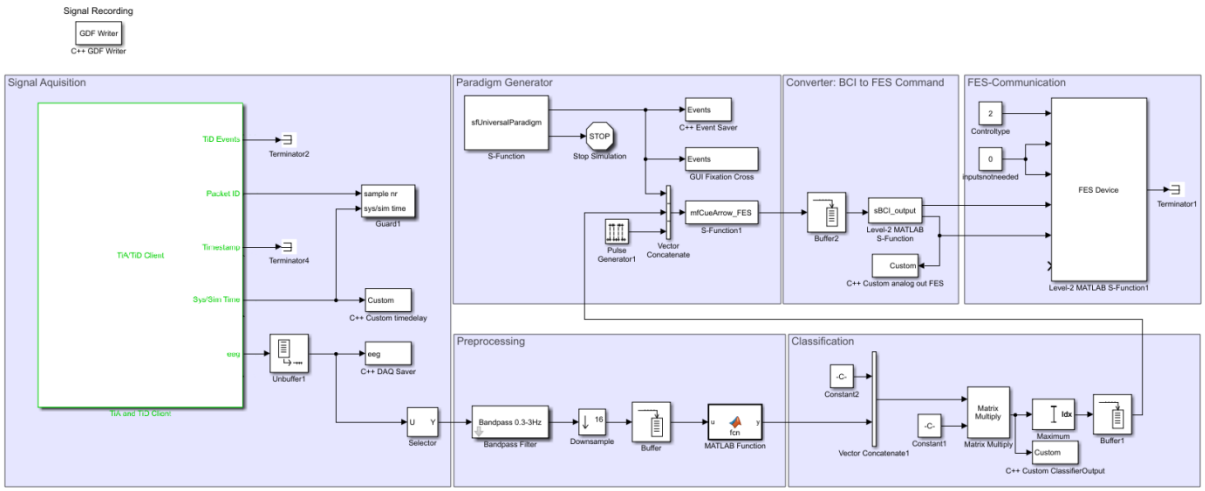

Figure 13: Simulink model for feedback with FES

For signal acquisition, a slightly modified version of the TOBI Signal Server and Client [40] was used. It is an interface to include several input systems, such as in this case the EEG-signal from the BBT EEG cap [41]. Additional, for paradigm generation, parts of the Biosig toolboox [42] and other Graz BCI libraries were applied and modified. All other aspects according the EEG processing are described in a more detailed way within the next chapters.

Paradigm

Following the preparations, the measurement was started. The paradigm and the study procedure are visualized in Figure 14 and Table 3. A cross and a sketch of the movement appeared in the middle of the screen indicating the start of a trial. Participants were instructed to focus on that cross and avoid blinking, eye movements, teeth clenching and other movement artefacts. Two bars were moving to finally reach the mid of the cross after 2.5 s, signalizing the participant to start the movement. They were instructed to execute the movements (palmar or pronation) for a minimum time of 2 s and then move back to the rest position. For the tetraplegic participant it was not possible to execute the palmar grasp and therefore, he had to attempt the movement. After 3-4 s the screen went black again and a break of 3 to 3.5 s was done to enable blinking. For each participant also a minimum of 3 rest runs were executed, where a green cross is visualized on the screen for 120 s and they were instructed to focus on that cross and try to minimize the amount of artefacts during this period. After four training runs (80 trials per class) and 3 rest runs the classifier calculation needed approximately 6-10 min. During this period a fine tuning of the FES-parameters took place. Including the initial configuration and this fine tuning, the configuration of the FES-parameters took about 30 min. For the test runs with feedback even a laughing or a sad smiley showed up, depending on the correct or wrong classification of the movement. A total amount of 40 trials per class were measured with feedback and thereafter 10 trials per class were recorded with FES-feedback. For the stimulation feedback the period where the smiley showed a correct classification was used to initialize a grasp by stimulation of the hand. In case of the palmar grasp, the stimulation started the grasp by opening the hand, followed by closing and opening again. For the pronation the hand was straightened first and then rotated and straightened again. This stimulation procedure took 10 s each.

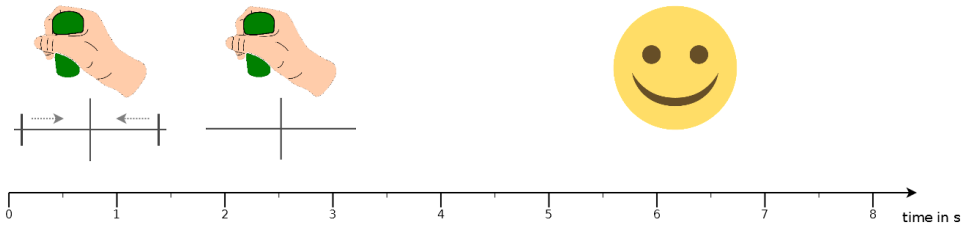

Figure 14: Paradigm timeline

Table 3: EEG – Experiment procedure

Nr.	Type	additional information
1	Preparation	Instruction / EEG-mounting + signal check / FES electrode mounting
2	Rest	120 seconds of rest
3	Training 1	Palmar/pronation – 40 Trials
4	Training 2	Palmar/pronation – 40 Trials
5	Rest	120 seconds of rest
6	Training 3	Palmar/pronation – 40 Trials
7	Training 4	Palmar/pronation – 40 Trials
8	Rest	120 seconds of rest
9	Calibration	Classifier Calibration / FES-electrode placement – fine tuning
10	Feedback 1	Palmar/pronation – 20 Trials
11	Feedback 2	Palmar/pronation – 20 Trials
12	Rest (optional)	120 seconds of rest
13	Feedback 3	Palmar/pronation – 20 Trials
14	Feedback 4	Palmar/pronation – 20 Trials
15	Feedback FES 1	Palmar/pronation – 10 Trials
16	Feedback FES 2	Palmar/pronation – 10 Trials

2.5.2 Artefact Handling

The most efficient way to handle artefacts is to carefully instruct the participants. Due to that, a detailed instruction was given to inform them, how they should behave during the experiment. Of course, not every individual is able to avoid blinking or other movements in the same way and additionally to that, there are also possible other influences from the environment like power noise, which results in artefacts in the EEG-signal. Because of this reason, artefact rejection was performed prior to the classifier calibration. Before epoching each trial from 1.5 s before to 2.5 s after the movement onset a 4^{th} order Butterworth zero phase bandpass filter between 0.3 Hz to 70 Hz was applied on the temporary signal. For the rejection three different methods from the EEGLAB package [43] were used. The first one simply marks all trials where values above and below a certain threshold are present (used threshold: 100 µV for upper and lower threshold). The other two methods mark trials with divergent joint probabilities and divergent kurtosis. For this, a threshold of 5 times the

standard deviation of the mean was used. All the marked trials were removed before further processing takes part.

2.5.3 Preprocessing and Feature Extraction

Raw EEG was filtered between 0.3 to 3 Hz with a 4th order causal Butterworth filter, following a downsampling of the signal to 16 Hz. As features for the classification, every second sample of this downsampled data was considered. With a defined window size of one second, each feature vector contained 288 features (32 channels x 9 sample points). The feature extraction approach and the optimal time window are based on the findings of [44].

2.5.4 Classification

The used classification method is based on shrinkage linear discriminant analysis (sLDA). Explanation of the LDA is based on [45]. LDA is a robust classification method and offers a linear decision surface where classes are separated by a linear function. Equation (3) shows the simplest linear discriminant function.

$$y(\boldsymbol{x}) = \boldsymbol{w}^T\boldsymbol{x} + \omega_0 \tag{3}$$

$\boldsymbol{w}$	weight vector
ω_0	bias
$\boldsymbol{x}$	input vector

Depending on $y(\boldsymbol{x})$, the vector $\boldsymbol{x}$ can be classified as class 1 if it is bigger or equal zero or vice versa for class 2, following the hyperplane definition at $y(\boldsymbol{x})$ = 0. The weight vector $\boldsymbol{w}$ is orthogonal to every vector on the decision surface, which means that $\boldsymbol{w}$ identify the orientation of the surface, and the location of the decision surface is associated with the bias ω_0.

The perpendicular distance to the decision surface can be stated as r.

$$\mathrm{r} = \frac{\mathrm{y}(\boldsymbol{x})}{\|\boldsymbol{w}\|} \tag{4}$$

For the fisher's linear discriminant analysis, the dimensionality gets reduced, which results in case of 2 classes in a reduction to one dimension.

$$\mathrm{y} = \boldsymbol{w}^{\mathrm{T}}\boldsymbol{x} \tag{5}$$

Of course, this dimensionality reduction causes a loss of information. Data which was discriminable in the higher dimensional representation can now overlap in the new

projection. A maximization of the class separation information has to be done by adjusting the components of the weight vector. A simple measure of the separation in the projection is represented by the class means. Though, only maximizing the difference of the class means for the new projection could lead to a high overlap too and therefore also the class variances are considered. This means that the maximization function should result in a large separation of the class means as well as in a small variance within each class. The fisher criterion $\mathrm{J}(\boldsymbol{w})$ define this ratio of the between-class variances $(\mathrm{m}_2 - \mathrm{m}_1)^2$ means and the within-class variances $s_1^2 + s_{2^2}$.

$$\mathrm{J}(\boldsymbol{w}) = \frac{(\mathrm{m}_2 - \mathrm{m}_1)^2}{\mathrm{s}_1^2 + \mathrm{s}_2{}^2} \tag{6}$$

m_1, m_2	mean of each class
s_1, s_2	within class variances
$\mathrm{J}(\boldsymbol{w})$	fisher criterion

To emphasize the dependency on the weight factor $\boldsymbol{w}$ the fisher criterion can be rewritten to:

$$\mathrm{J}(\boldsymbol{w}) = \frac{\boldsymbol{w}^{\mathrm{T}} \boldsymbol{S_B} \boldsymbol{w}}{\boldsymbol{w}^{\mathrm{T}} \boldsymbol{S_W} \boldsymbol{w}} \tag{7}$$

$\boldsymbol{S_B}$	between-class covariance
$\boldsymbol{S_W}$	within-class covariance

A differentiation with respect to $\boldsymbol{w}$ and then neglecting the scalar factors, because only the direction of the weight factor $\boldsymbol{w}$ and not the magnitude is important here, results in following statement:

$$\boldsymbol{w} \propto \boldsymbol{S_W^{-1}}(\mathrm{m}_2 - \mathrm{m}_1) \tag{8}$$

For an isotropic within-class covariance $\boldsymbol{S_W}$, the weight factor $\boldsymbol{w}$ is proportional to the difference of the class means. This is the fisher linear discriminant and can be used to find a threshold y_0, which is in the 2-class case a point in the projected one-dimensional space and should discriminate these 2 classes.

The supplementary shrinkage describes a type of regularization, which is added to tune the covariance matrix. Usually the empirical covariance is taken as an estimator for the estimation of the covariance matrix. In case of high dimensional data and only few data points, the calculation becomes inaccurate. The consequence is a decreasing classification performance. The regularized shrinkage covariance matrix has the same eigenvectors than

the standard form but modifies extreme eigenvalues in a way that the calculations lead to a better classification performance. [46]

The experimental design requires to find the best time point for classification, consequently a cross validation was performed for every timepoint. The cross validation should give a good estimate on how the classifier will perform in an online scenario for defined time windows. Within a defined region for every timepoint and its corresponding features the sLDA were repeatedly trained and tested with a repeated k-fold cross validation. Due to limited time and computational power during the study a good balance for the cross validation was given by using 5x5 cross validation from 0 s to 2 s with respect to the movement onset. Since the features are extracted from a dataset of 1 s, the most discriminable patterns are assumed within this time period.

2.5.5 Data Analysis

In this section the additional data analysis methods which are used for offline analysis, visualization and statistical testing are shortly described.

Significance level

The classification accuracy alone does not implicit indicate whether the classifier really works better than a random classification. For 2 classes, like throwing a coin, the chance level is at 50 percent. This is only the truth for an infinite number of samples which is of course just theoretically possible. For real experiments this chance level should be investigated with a confidence interval depending on the number of trials and the selected level of α. For this thesis an adjusted Wald interval calculation with an α of 0.05 were used to calculate this significance threshold. [47] [48]

Rest-trial Extraction

All measured rest trials were further used to test classification performances of movement versus rest conditions. This is done by epoching trials from the rest runs. The first 10 seconds of each rest run were cut out and, depending on the analysis, with the remaining signal a specified number of rest trials were created to train a classifier in the same way as it is trained in the movement versus movement condition. The epoched rest trials were, of course, not affected by the artefact removal to get a realistic output, more specifically to prevent falsification of the analysis. An unbalanced classifier, which means that more rest trials are taken for the training of the classifier, was used. More precisely, 270 rest trials

were used, whereas for the movement condition, both grasps were summed, which ended in the same number of trials which is stated in Table 5 and is in average approximately half the number of rest trials.

Classifier Output – smoothing

The output of the classifier had a sampling rate of 16Hz. This means, every 62,5 ms a sample is created. Due to the fact that a human is not able to react and move that constant to an external stimulus also the possibility of smoothing the classifier output over a specified time period and the result on the classification accuracy was investigated. This smoothing is done by averaging the given classification output over a specified number of samples. Different numbers of samples (±1 to ±8) were compared according to their classification performance.

Common Average Reference

For visualization and analysis of the MRCP's a common average reference (CAR) was applied, which is a common method for EEG-signal processing. This method simply subtracts the mean of all electrodes from the signal of each electrode, done for each time point. By using CAR, it is presumed that activities which occur at the same time over all electrodes must be artefacts and therefore can be eliminated. [49]

3. Results

3.1 Functional Electrical Stimulation Evaluation

The evaluation of the FES and furthermore of the grasps was done during the experiment. All measured participants, including the SCI, were able to perform the palmar grasp with electrical stimulation only. They managed to hold the cylindrical object (see Figure 16) easily. Also, it was possible to stimulate the M. pronator teres efficiently enough to pronate the arm. For 5 out of 10 healthy people and for the person with SCI it was not possible to efficiently stimulate the M. brachioradialis. Therefore no back-rotation to the initial position could be performed.

In Table 4, the configured amplitude values for each muscle group and the possible movements per participant are stated. The frequency was defined as 23 Hz and the maximum pulse width fixed to 500 µs.

Table 4: Stimulation values of participants and possible grasps to perform, * in backrotation marks participants where only simulated feedback was given for that grasp

Participant	Amplitude value in mA					Grasp patterns			
	Thumb abduction	Hand Flexion	Hand extension	Pronation	Back-rotation	Palmar Grasp	Hand open	Pronation	Back rotation
GRZ003 (SCI)	13	14	12	15	12	✓	✓	✓	✗
DQ9	7	10	10	11	6*	✓	✓	✓	✗
ED4	11	12	12	15	16	✓	✓	✓	✓
EH2	7	12	11	12	7*	✓	✓	✓	✗
EH7	11	10	13	12	14	✓	✓	✓	✓
EH8	8	6	10	13	6*	✓	✓	✓	✗
EH9	13	11	13	14	16	✓	✓	✓	✓
EI8	5	12	12	11	6*	✓	✓	✓	✗
EI9	7	13	11	12	6*	✓	✓	✓	✗
EJ3	9	11	13	9	8	✓	✓	✓	✓
EJ4	8	9	15	8	8	✓	✓	✓	✓

Following grasp maps (Figure 15) ensure the best grasp patterns according to the experimental outcome. Some representative examples of hand states during specific stimulations are shown in Figure 16.

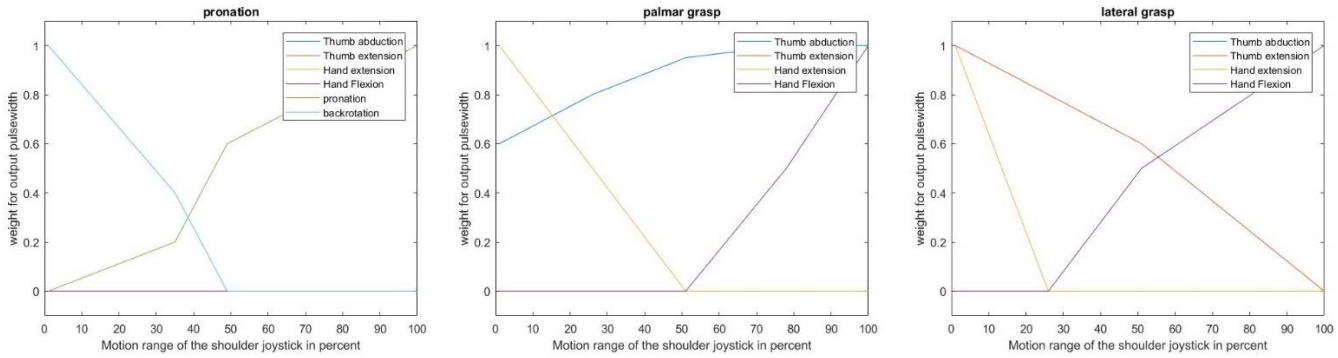

Figure 15: Default grasp maps, left to right: pronation, palmar and lateral grasp

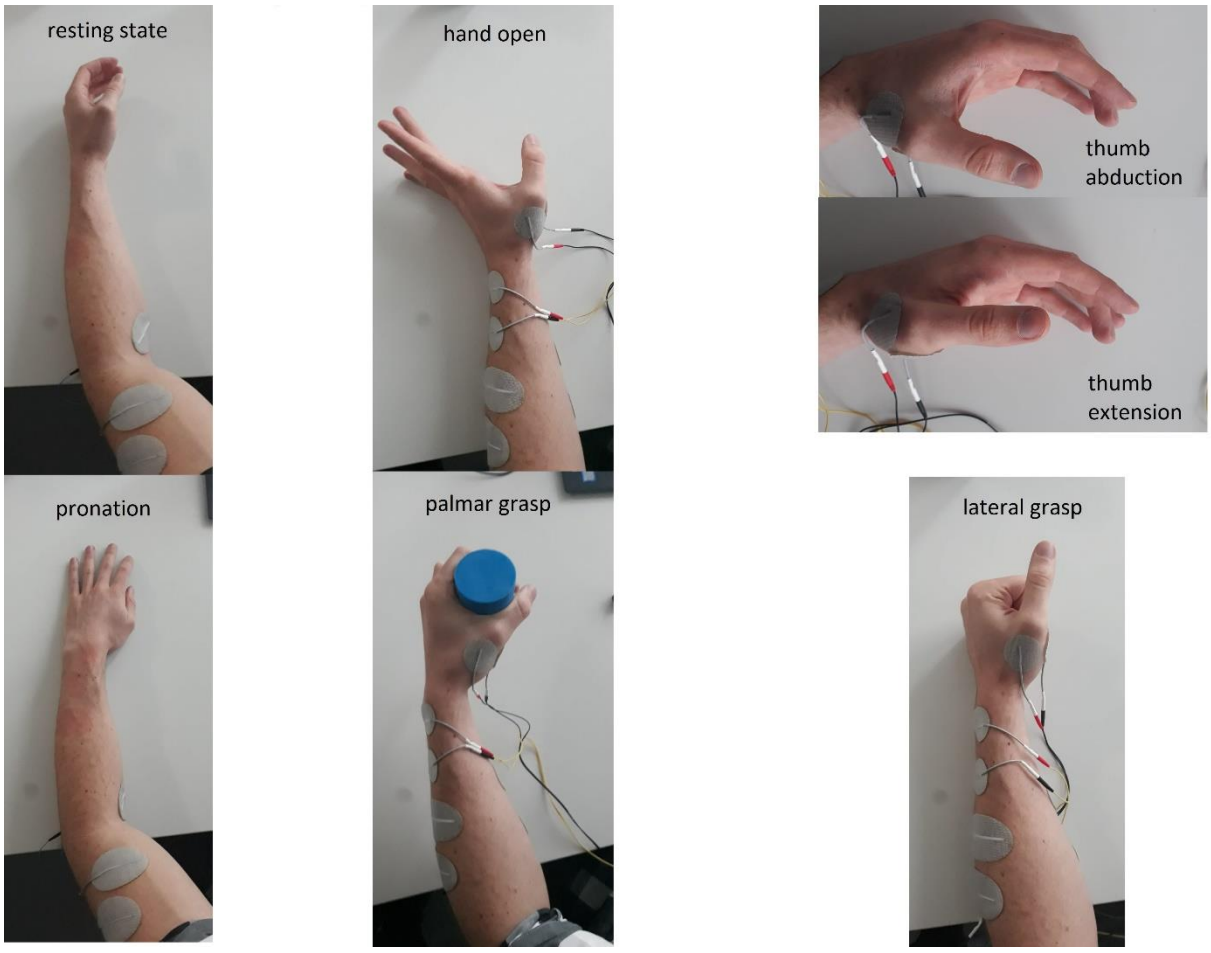

Figure 16: Hand positions during grasp stimulation. Left: up – rest position, down – rotated position, middle: up - hand open, down: palmar grasp, right: up – difference between thumb abduction (upper picture) and thumb extension(lower picture), down – lateral grasp

3.2 Shoulder Position Sensor

All healthy participants were able to control the sensor output efficient with only small changes to the default configuration. Also, the participant with an SCI produced only a negligible number of false commands. But, there was a longer preconfiguration of the movement areas necessary, due to the lower motion range. The visualization of the current

position on the screen improved the performance from the beginning and enabled the participants to adapt their movements according to the mode of operation.

3.3 EEG-Study

Results of the EEG part show how the classifier performed on- and offline and also point out the EEG-specific patterns obtained with the preprocessing steps explained in the last chapter.

Overall, the stability and performance of the system was constant during the whole study. Preliminary tests showed a constant delay between the appearance of the cue on the screen and the system of about 148 ms with a standard deviation of about 16 ms due to the Bluetooth communication. This delay did not increase for the appliance of the feedback systems with and without FES-device.

3.3.1 Online Cross-Validation Results and Classification Evaluation

To begin with, the cross-validation results for all participants at different time points are visualized in the following figures (Figure 17 - Figure 27). At the timepoint 0 s, the participants were instructed to execute the movement. The classifier indicated by the red dot, was further used for the online feedback. This is the timepoint where the classification accuracy reaches its maximum.

An overview of the classification results is given in Table 5. The * marks measurements, where the artefact detection removed more than ¼ of all trials and was therefore adapted (EI9 – smaller artefact rejection window) or rather skipped (EH2).

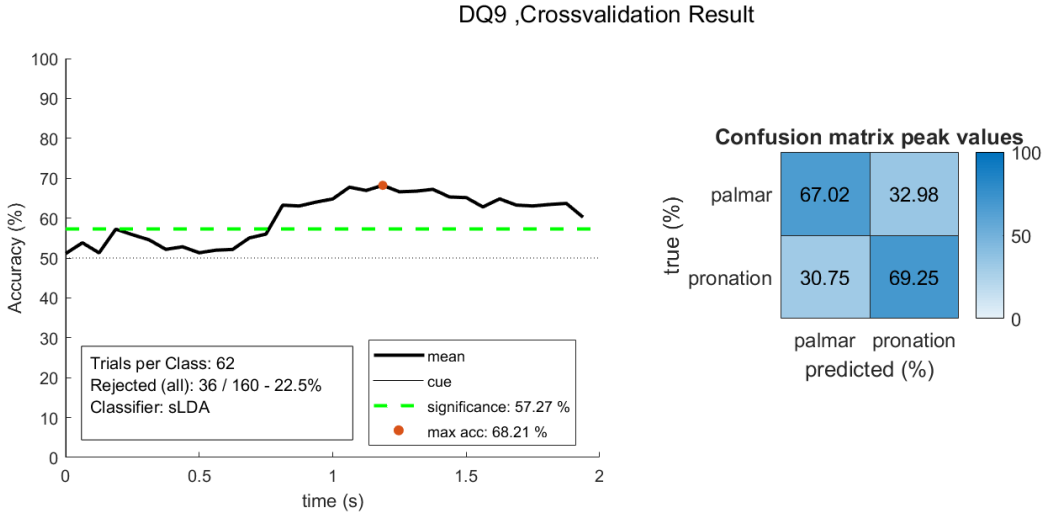

Figure 17: 5 x 5 Cross-validation result for participant DQ9 with the associated truth table, online study - training runs

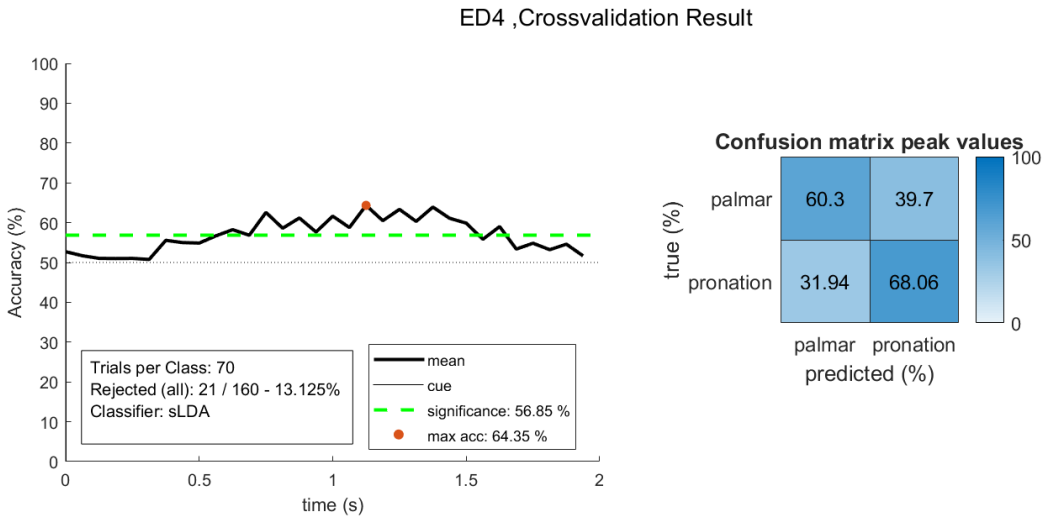

Figure 18: 5 x 5 Cross-validation result for participant ED4 with the associated truth table, online study - training runs

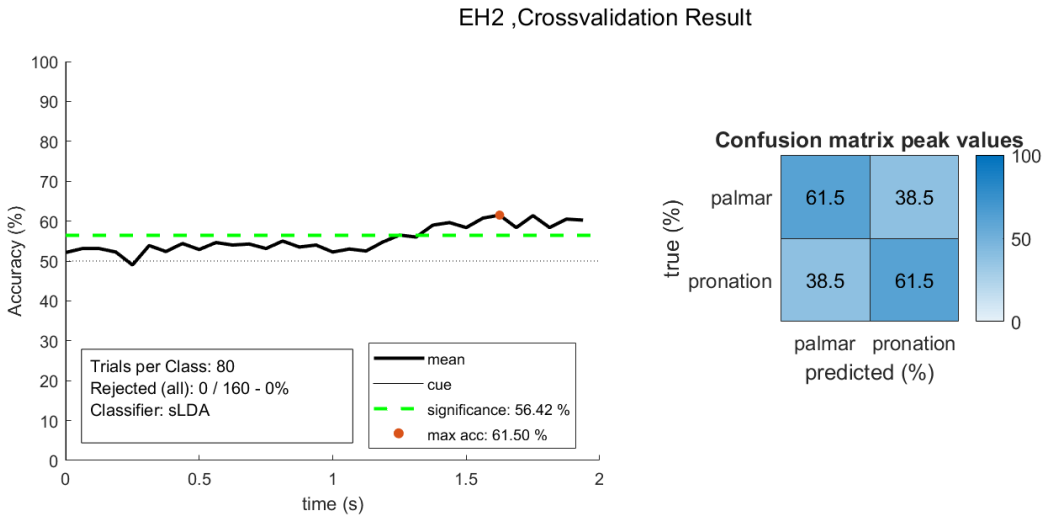

Figure 19: 5 x 5 Cross-validation result for participant EH2 with the associated truth table, online study - training runs

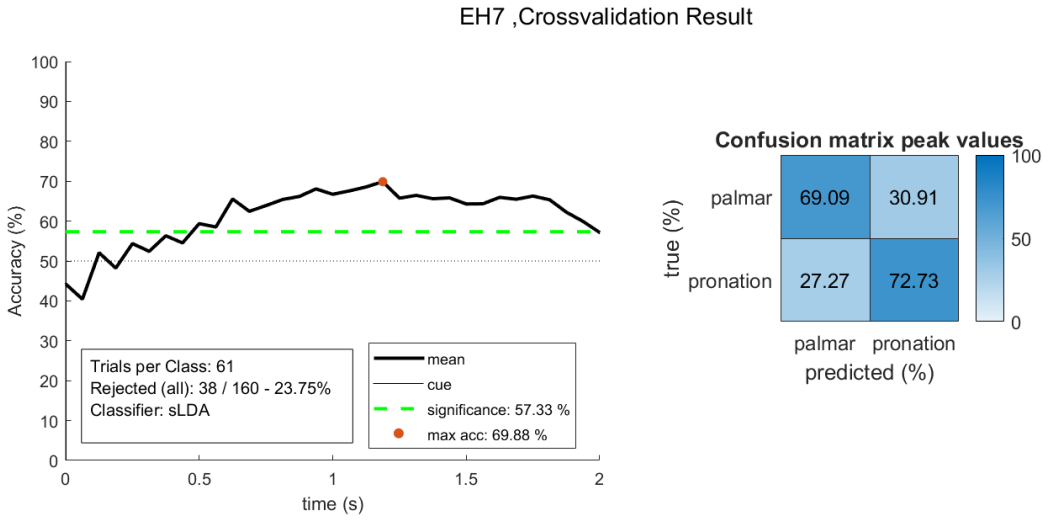

Figure 20: 5 x 5 Cross-validation result for participant EH7 with the associated truth table, online study - training runs

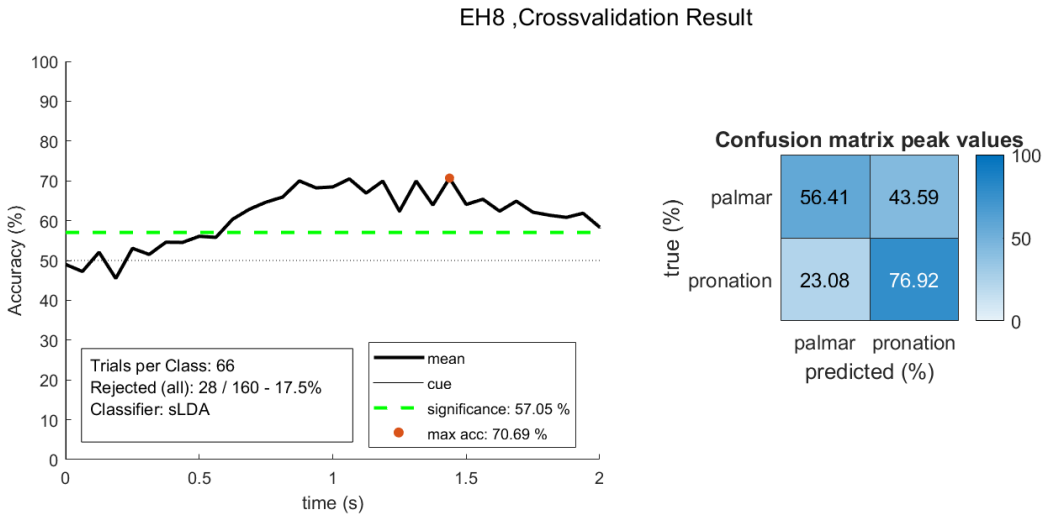

Figure 21: 5 x 5 Cross-validation result for participant EH8 with the associated truth table, online study – training runs

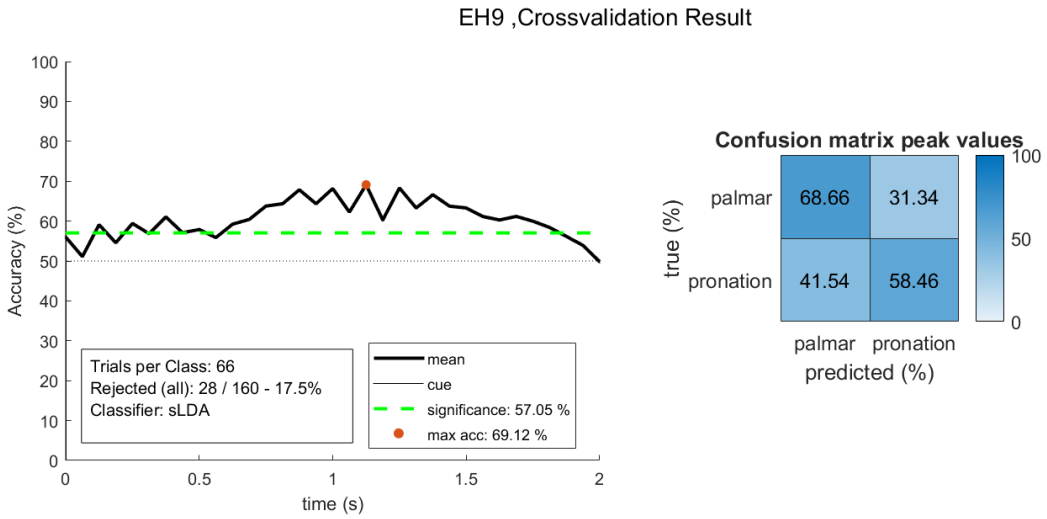

Figure 22: 5 x 5 Cross-validation result for participant EH9 with the associated truth table, online study - training runs

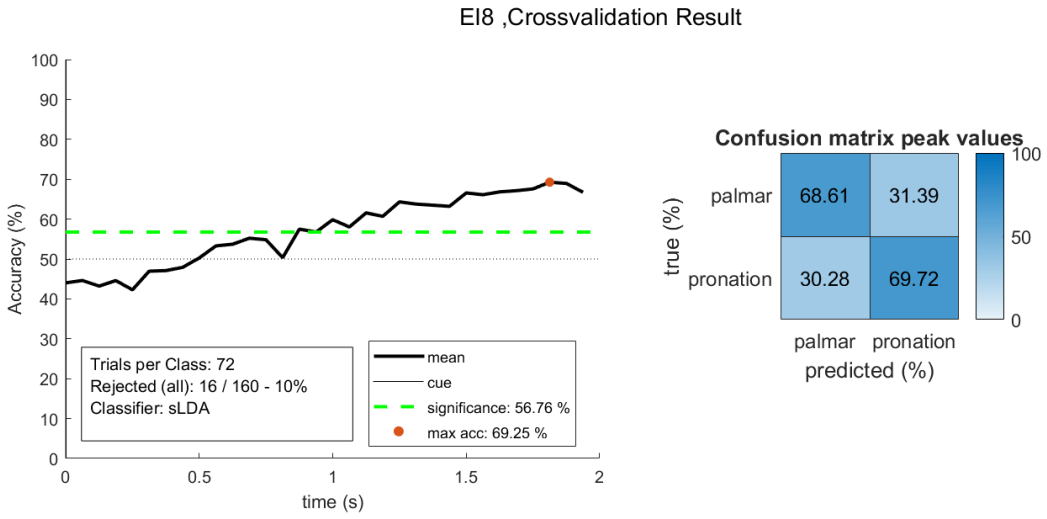

Figure 23: 5 x 5 Cross-validation result for participant EI8 with the associated truth table, online study -training runs

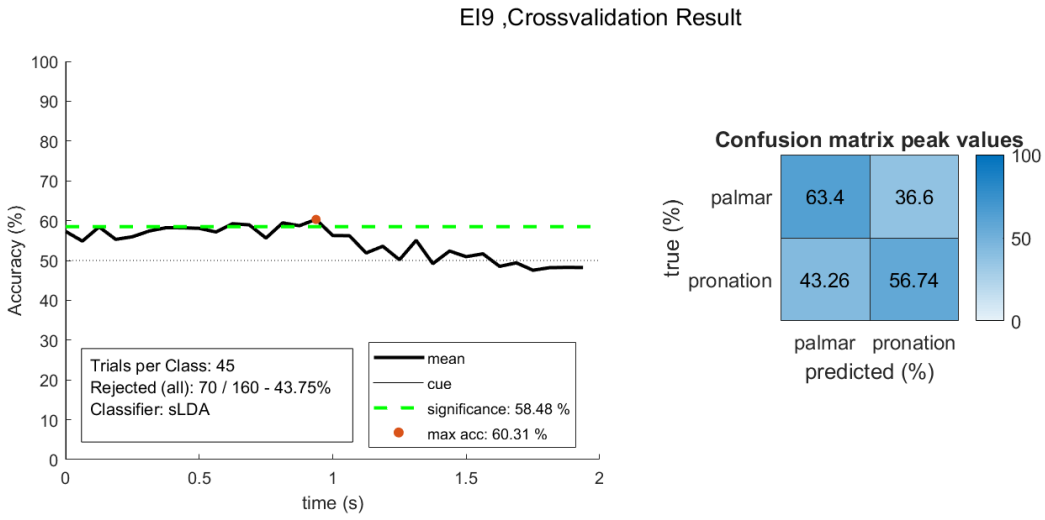

Figure 24: 5 x 5 Cross-validation result for participant EI9 with the associated truth table, online study - training runs

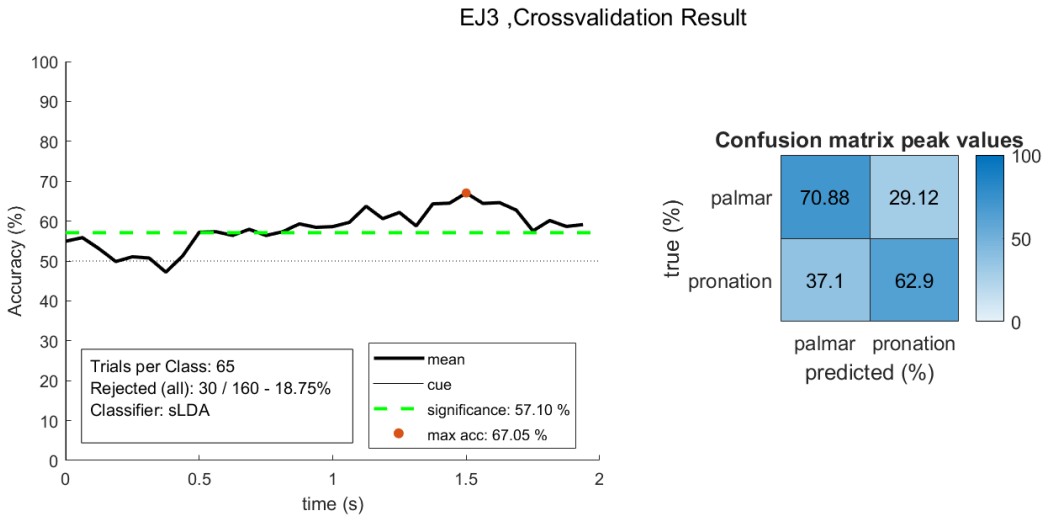

Figure 25: 5 x 5 Cross-validation result for participant EJ3 with the associated truth table, online study - training runs

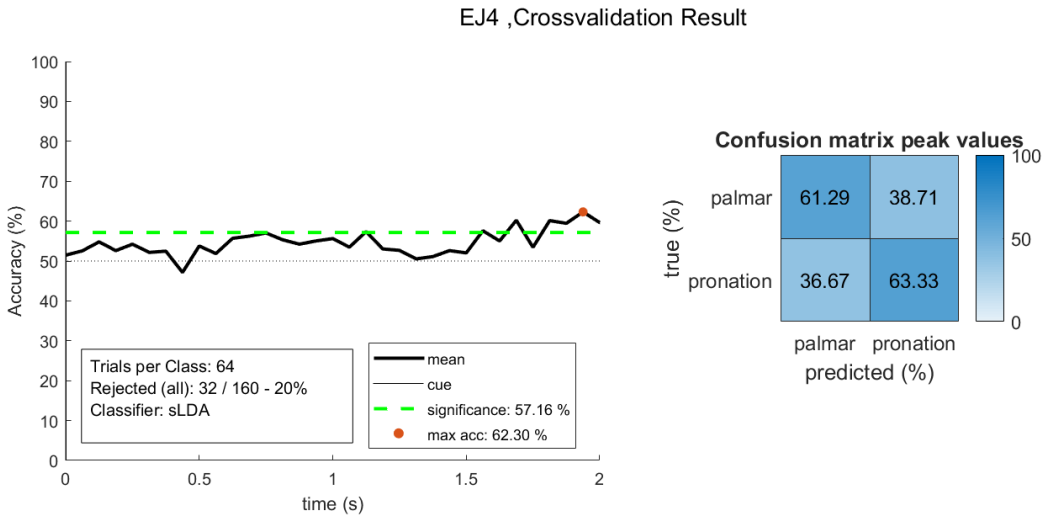

Figure 26: 5 x 5 Cross-validation result for participant EJ4 with the associated truth table, online study - training runs

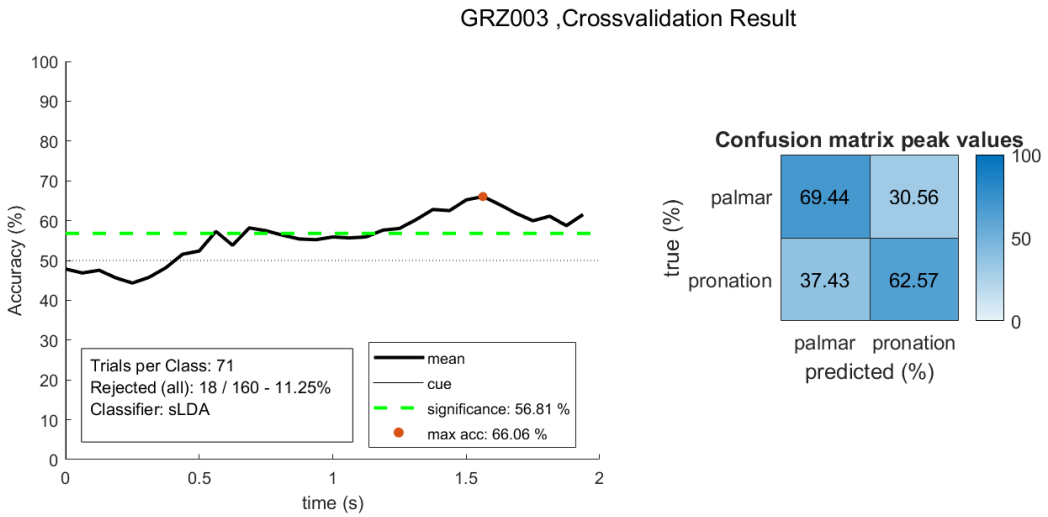

Figure 27: 5 x 5 Cross-validation result for participant GRZ003 with the associated truth table, online study - training runs

Table 5: Overview of Classification Results – timepoint, Accuracy and number of trials, online feedback significance level 58 % (100 trials, α=0.05, adjusted Wald interval)

Participants	Cross Validation		Online Feedback Accuracy in %	Classification Timepoint in s	Number of trials
	Max. accuracy in %	Significance level in %			
DQ9	68,21	57,27	58	1,2500	124
ED4	64,35	56,85	67	1,1875	139
EH2	61,50	56,42	49	1,6875	160*
EH7	69,88	57,33	70	1,2500	122
EH8	70,69	57,05	65	1,6250	132
EH9	69,12	57,05	61	1,3125	132
EI8	69,25	56,76	65	1,8750	144
EI9	60,31	58,48	66	0,9375	90*
EJ3	67,05	57,10	68	1,5625	130
EJ4	62,30	57,16	51	2,0000	128
GRZ003	66,06	56,81	64	1,6250	142
Average	66,25	57,12	62,18	1,4830	131,18

Next, the online classification of the single feedback trials for each timepoint during a trial is presented. The classification timepoint is indicated by a black line, whereas trials 1-40 represent the feedback trials without and 41-50 with FES. Red areas outline classification of class 1 (palmar grasp) and turquoise areas of class 2 (pronation). Time axis starts again at the movement onset specified at 0.

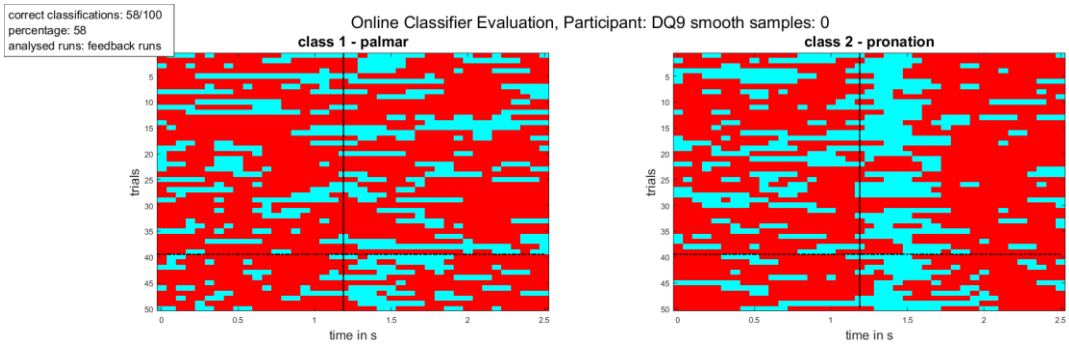

Figure 28: Classifier Output over time for participant DQ9, online study - feedback runs, red-palmar, blue-pronation, black vertical line: classification timepoint, FES-feedback trials below dashed horizontal line

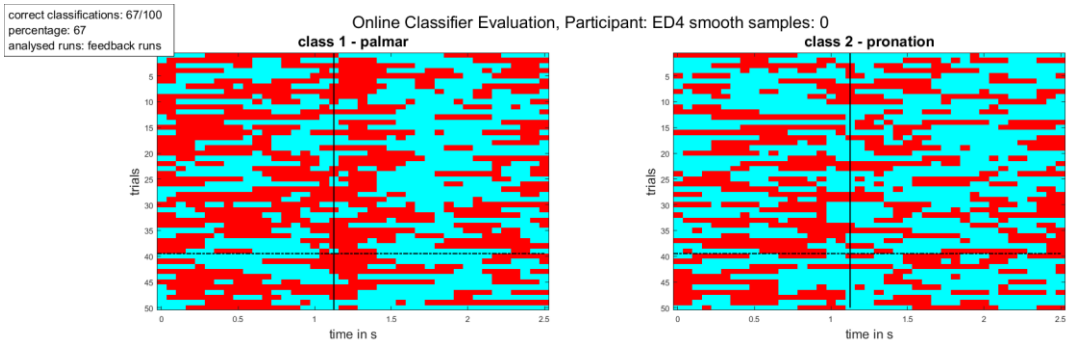

Figure 29: Classifier Output over time for participant ED4, online study - feedback runs, red-palmar, blue-pronation, black vertical line: classification timepoint, FES-feedback trials below dashed horizontal line

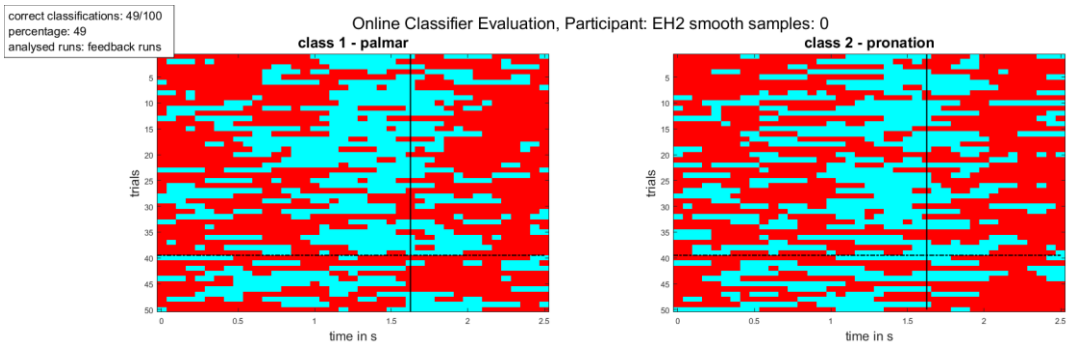

Figure 30: Classifier Output over time for participant EH2, online study - feedback runs, red-palmar, blue-pronation, black vertical line: classification timepoint, FES-feedback trials below dashed horizontal line

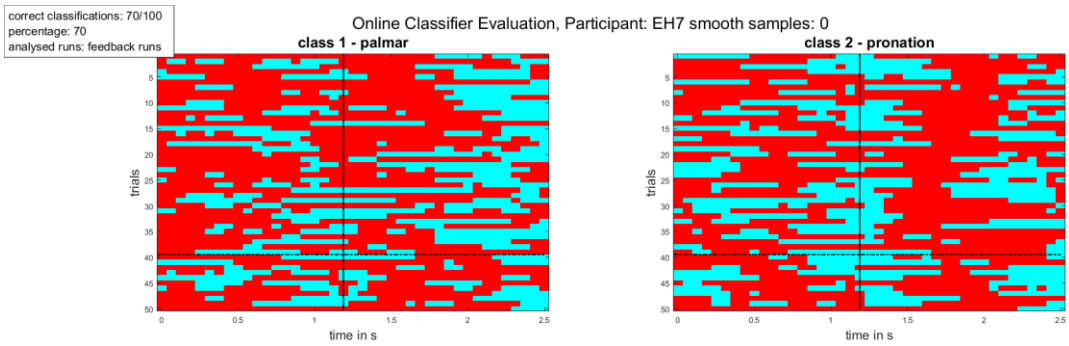

Figure 31: Classifier Output over time for participant EH7, online study - feedback runs, red-palmar, blue-pronation, black vertical line: classification timepoint, FES-feedback trials below dashed horizontal line

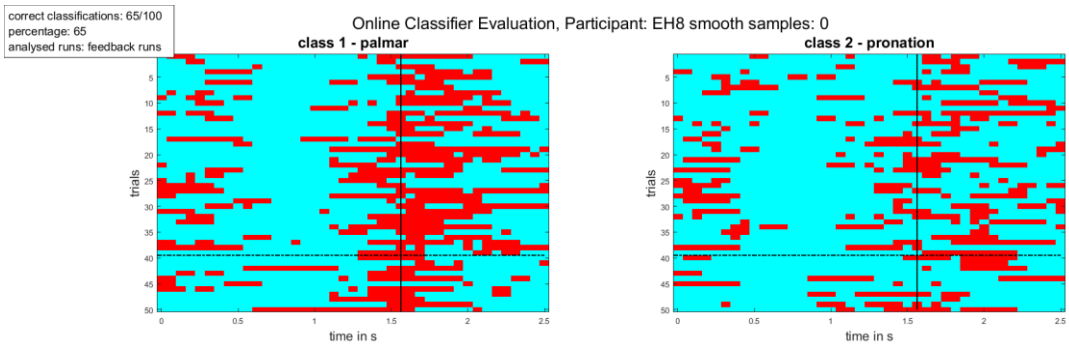

Figure 32: Classifier Output over time for participant EH8, online study - feedback runs, red-palmar, blue-pronation, black vertical line: classification timepoint, FES-feedback trials below dashed horizontal line

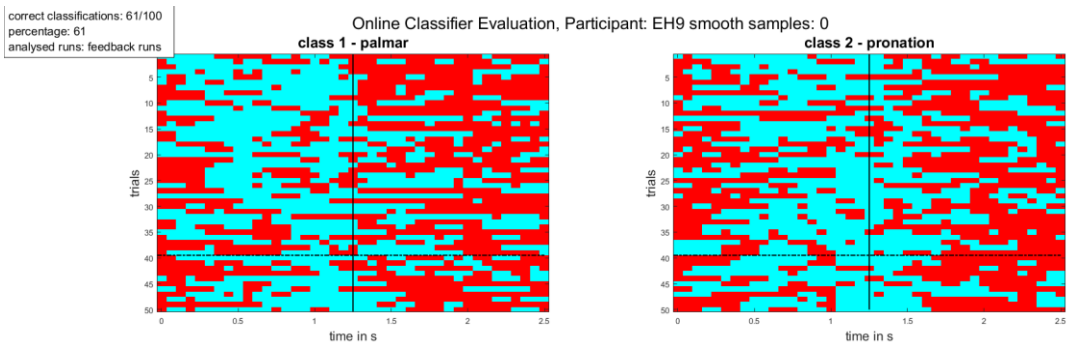

Figure 33: Classifier Output over time for participant EH9, online study - feedback runs, red-palmar, blue-pronation, black vertical line: classification timepoint, FES-feedback trials below dashed horizontal line

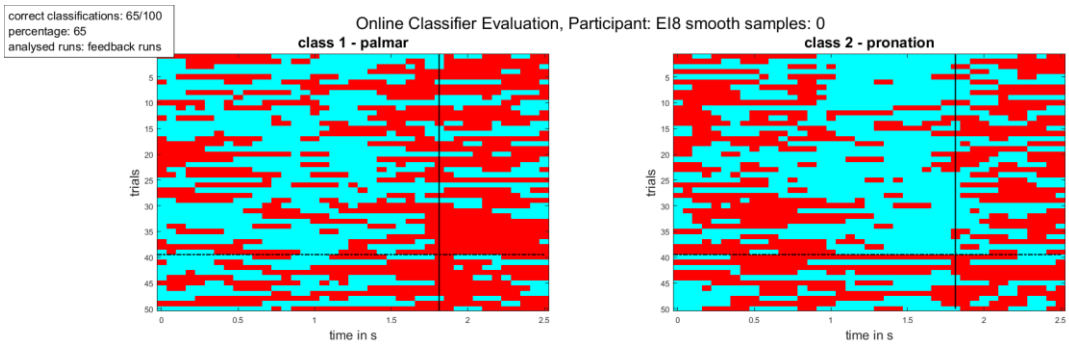

Figure 34: Classifier Output over time for participant EI8, online study - feedback runs, red-palmar, blue-pronation, black vertical line: classification timepoint, FES-feedback trials below dashed horizontal line

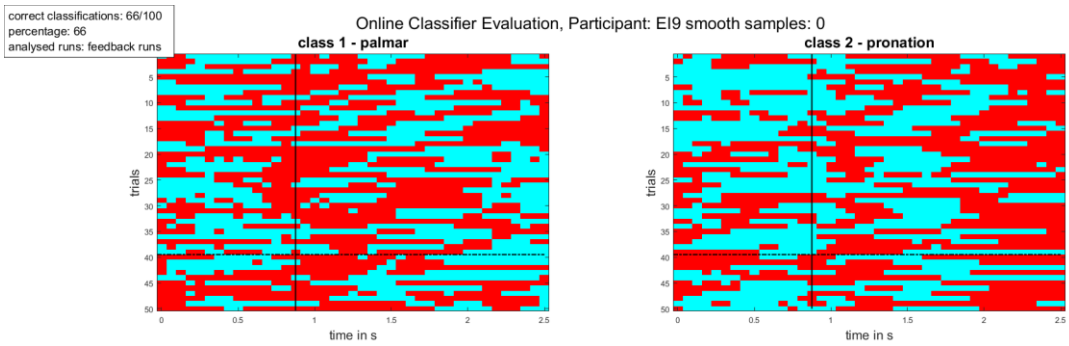

Figure 35: Classifier Output over time for participant EI9, online study - feedback runs, red-palmar, blue-pronation, black vertical line: classification timepoint, FES-feedback trials below dashed horizontal line

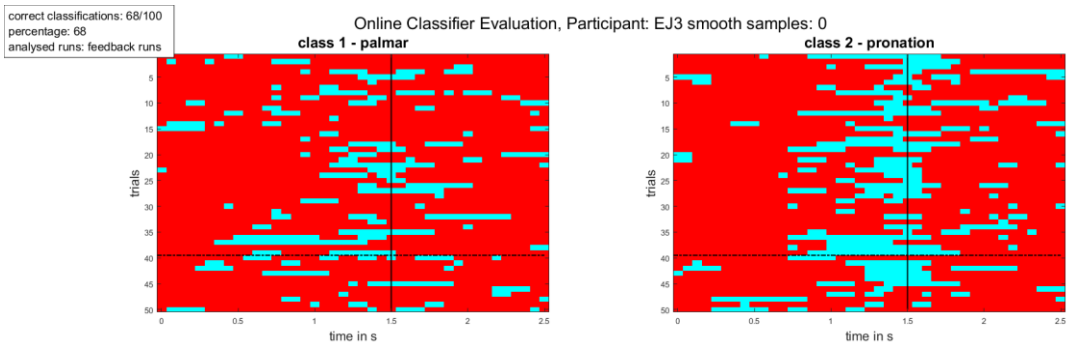

Figure 36: Classifier Output over time for participant EJ3, online study - feedback runs, red-palmar, blue-pronation, black vertical line: classification timepoint, FES-feedback trials below dashed horizontal line

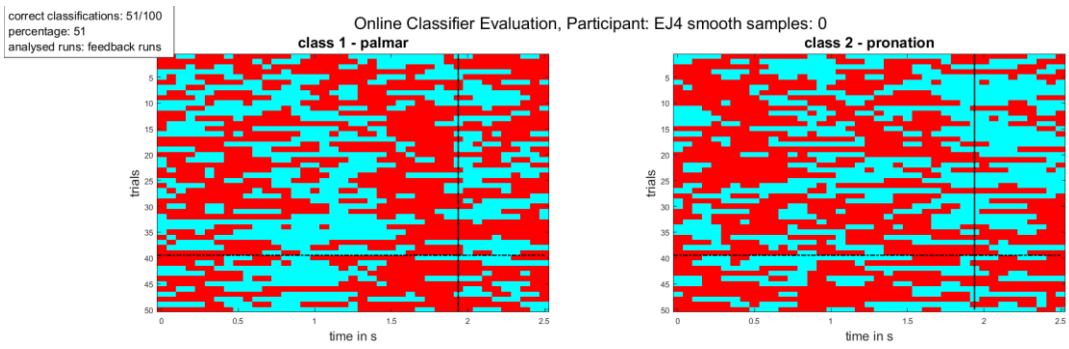

Figure 37: Classifier Output over time for participant EJ4, online study - feedback runs, red-palmar, blue-pronation, black vertical line: classification timepoint, FES-feedback trials below dashed horizontal line

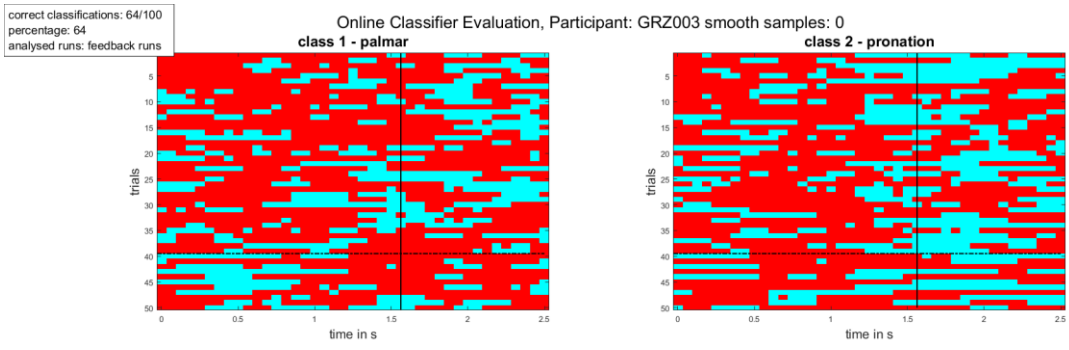

Figure 38: Classifier Output over time for participant GRZ003, online study - feedback runs, red-palmar, blue-pronation, vertical black line: classification timepoint, FES-feedback trials below dashed horizontal line

3.3.2 Movement-related-cortical potentials

The next figures contain the MRCP results for all participants and an illustrating example for one individual. Visualized is the comparison between the palmar and the pronation grasp. To show the dispersion of the signals the standard error of the mean was selected. For the visualization of the MRCP pattern an acausal filtering was applied. All other processing steps are equal to the preprocessing steps for the online study.

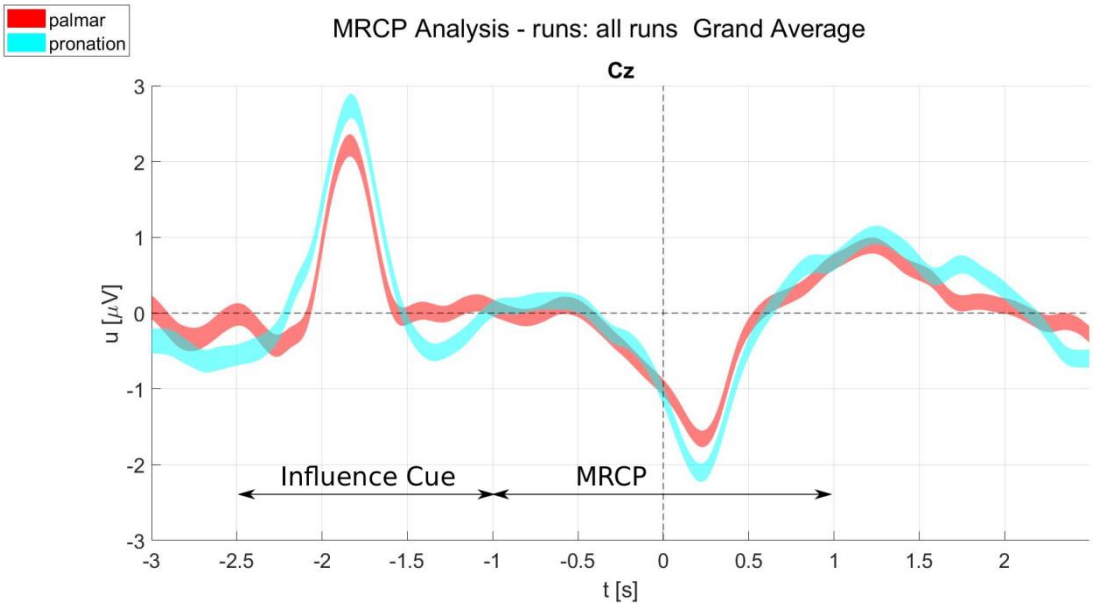

Figure 39: Grand average over all participants for all runs and electrode position Cz, CAR filtered, Interval: mean + standard error, second 0 defined as movement onset

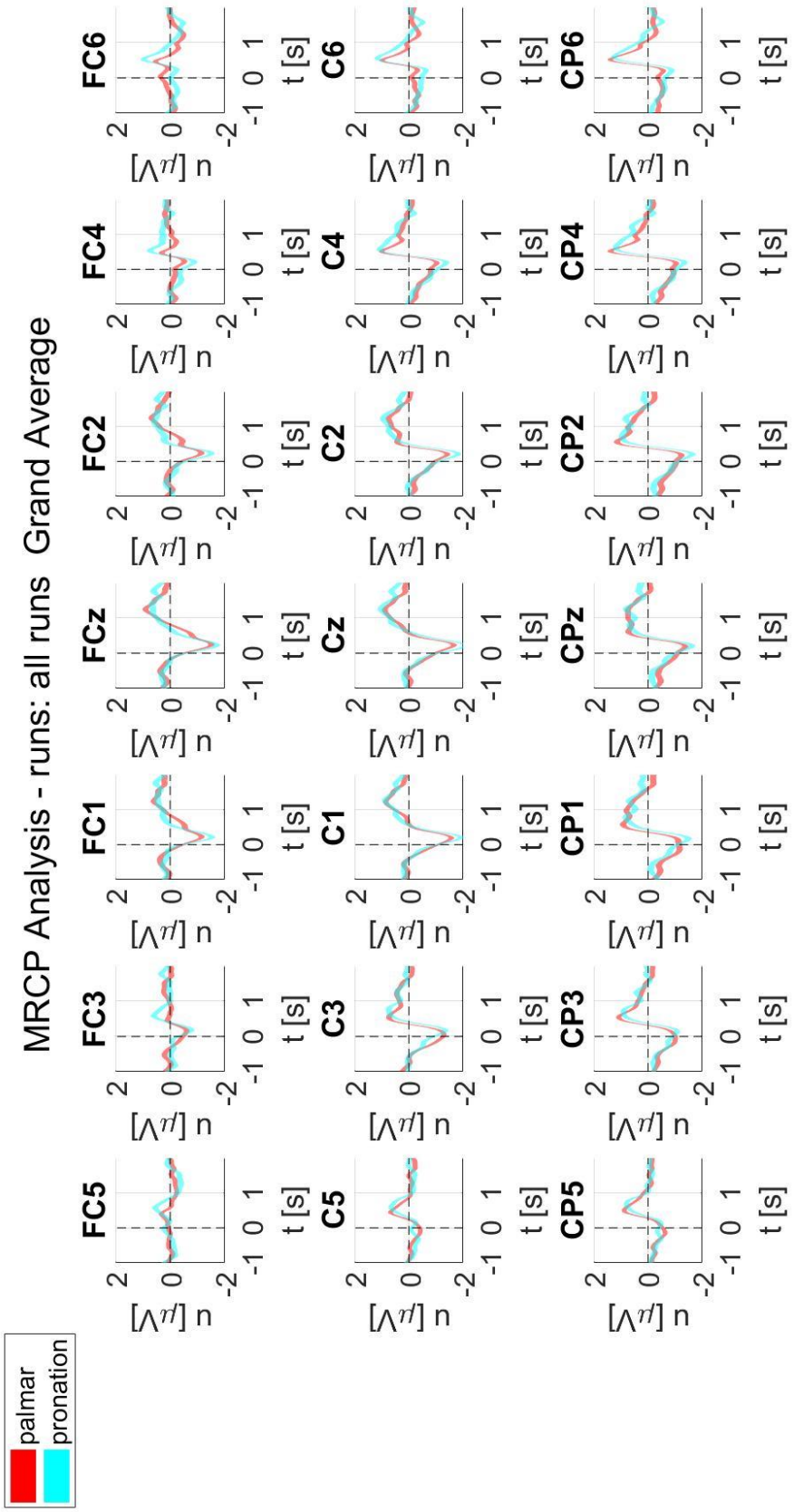

Figure 40: Differences of electrode positions with the grand average of all participants and all runs, CAR filtered, Interval: mean + standard error, second 0 defined as movement onset

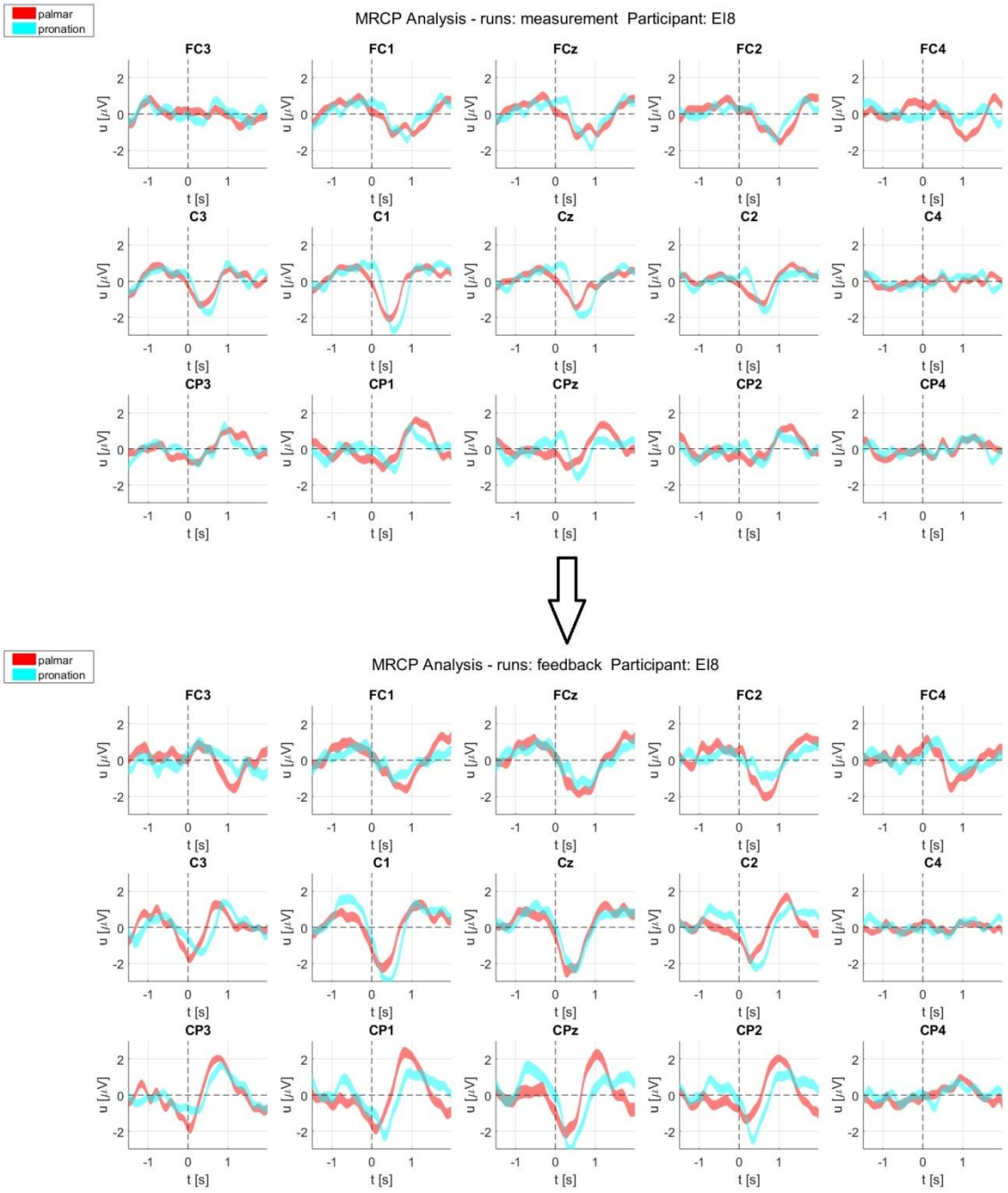

Figure 41: Participant EI8 training effect, CAR filtered, Interval: mean + standard error, second 0 defined as movement onset

3.3.3 Additional Data Analysis

The additional data analysis contains the smoothing effect on the overall performance of the classifier output and an evaluation of movement versus rest classification.

Table 6: Effect on feedback when smoothing the classifier output, sample rate of classifier output: 16 Hz

Participants	Additional smoothing of Classifier output								
	no smoothing	± 1	± 2	± 3	± 4	± 5	± 6	± 7	± 8
DQ9	58	56	53	58	57	57	56	57	57
ED4	67	64	68	67	67	64	60	61	62
EH2	49	51	52	54	54	54	53	50	52
EH7	70	61	61	65	64	64	63	63	58
EH8	65	71	69	67	67	67	69	67	66
EH9	61	59	60	60	59	58	60	61	62
EI8	65	66	72	73	76	77	73	75	74
EI9	66	66	69	65	65	68	60	62	61
EJ3	68	69	66	64	61	58	57	54	54
EJ4	51	61	61	65	65	65	66	68	67
GRZ003	64	61	63	62	64	64	64	61	61
Average	62,18	62,27	63,09	63,64	63,55	63,27	61,91	61,73	61,27

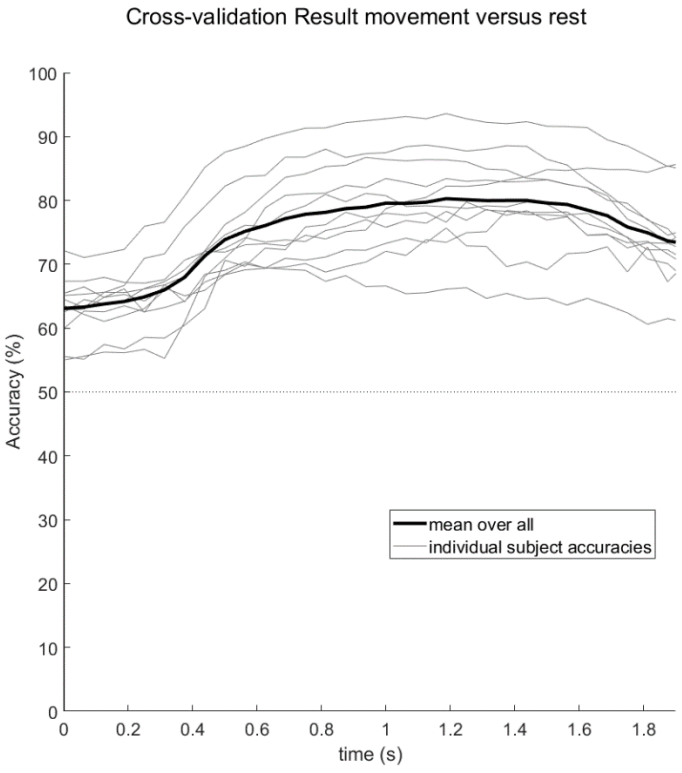

Figure 42: Average classifier cross validated accuracy output over all participants, rest versus movement condition – measurement runs

Table 7: Accuracies, true positive rates, false positive rates and timepoints for classification of movement versus rest analysis

Participants	Accuracy in %	TPR Movement in %	TPR Rest in %	FPR Movement in %	FPR Rest in %	Classification timepoint in s
DQ9	93,60	93,50	95,93	4,07	6,50	1,25
ED4	83,42	84,29	81,48	18,52	15,71	1,06
EH2	78,43	66,67	80,74	19,26	33,33	1,44
EH7	79,75	76,15	84,81	15,19	23,85	1,31
EH8	88,67	94,03	90,00	10,00	5,97	1,19
EH9	86,74	88,64	84,44	15,56	11,36	1,00
EI8	85,41	84,46	84,44	15,56	15,54	1,94
EI9	70,06	65,56	74,81	25,19	34,44	0,63
EJ3	81,10	80,77	82,22	17,78	19,23	1,00
EJ4	78,60	73,64	81,85	18,15	26,36	1,38
GRZ003	75,69	71,63	80,37	19,63	28,37	1,25
Average	81,95	79,94	83,74	16,26	20,06	1,22

4. Discussion

In this chapter, the results of the EEG-study as well as the performance of the neuroprosthesis system are discussed and possible future improvements of the system are listed.

4.1 Hardware / Software

As the hardware has a big impact on the performance of the system, a short discussion about the advantages/disadvantages is given here. For a neuroprosthesis, the Motion Stim 8 with the modified firmware provides a good basis to stimulate muscles for generation of specified grasp patterns. The communication via Bluetooth with the FESMUX showed big advantages in case of usability and mobility, which would make out-of-the-lab studies easy. Another benefit is the faster communication for the readout process of the shoulder position sensor because it is done by a microcontroller board and not by the Motion Stim 8. Anyway, a processing rate of 16 Hz is the tested output limit for the implemented neuroprosthesis because both, the Motion Stim 8 alone as well as the FESMUX are working stable in this range for most possible stimulation applications. The water based wireless EEG-cap from BBT also uses Bluetooth to connect to the CU. As it is stated in the results above, it works stable, although it results in a slightly bigger delay when comparing to wired EEG-systems. This higher delay causes no further problems for most applications, because it is stable over time and did not show significant higher fluctuations in comparison to a wired device. When connecting both Bluetooth devices at the same time, it rarely happened that the communication to a device broke down. This behavior was not further investigated because the appearance of it was neglectable.

The results of the EEG-study additionally show that the system is prone to external influences and to individual behavior of a participant. Albeit, the used water-based electrode cap has the big advantage of simplicity, the signal quality seems to be worse than for gel-based electrode caps. Especially for people with thick hair, it is hard to reach a signal quality where external influences could be reduced to an acceptable limit. Also, due to the decrease of signal to noise ratio, the classification performance is lower than for similar studies with gel-based systems [37] [44]. This result is also described in literature [50] [51].

4.2 Neuroprosthesis

The neuroprosthesis parameters are given in Table 4. It is shown that all participants were able to perform the palmar grasp, hand open as well as the pronation. The stimulation of the M. brachioradialis, which is responsible to return the hand position back to its neutral position, only worked with 5 out of 11 participants without additional modifications. The reason is that this muscle and its origin lies hidden between two bigger muscles, the M. triceps brachii and the M. biceps brachii. Though, for all participants, a sufficient function of this rotation back to the neutral position could be reached when the electrode gets pressed on the skin. This means it is possible to rotate the arm back from the pronation state by adding a bandage or similar objects to press the electrode at the right position onto the skin surface. In Figure 15 and Figure 16, especially the difference between the palmar grasp and the lateral grasp with respect to the thumb stimulation need to be highlighted. For the palmar grasp, the thumb must be abducted before the closing of the hand to efficiently grasp a cylindrical shape. As already mentioned, all muscles were stimulated without an antagonist. These results in a more or less on/off grasp pattern, where it is not possible to stay in a state in between for a longer period. This approach is simpler to configure and needs less electrode pairs on the limited space of the arm. The examples of real hand stimulation (see Figure 16) point out the most representative hand states, used to control the arm via the neuroprosthesis. As it can be seen, the stimulation results in efficient grasps for the specified task. Even though the grasp pattern does not look exactly the same as the grasp pattern of a healthy person, people are able to grasp for example a can or to rotate their hand to the desired position. For these tests of the neuroprosthesis grasp pattern only, the control was done with keyboard-inputs.

4.3 Shoulder Position Sensor

The shoulder position sensor is an efficient and easy way to control a neuroprosthesis. Although, even for this simple shoulder movements a training is necessary, because by moving the arm and execute grasps, involuntary movements of the opposite shoulder need to be decreased. Also, it seems to be of high importance that a user fully understands the real working principle of the joystick position sensor, otherwise the consequence is demotivation due to an unnecessarily long preconfiguration phase. Additional influence factors are the small range of motion, especially for tetraplegic users, and the unwanted rotation due to the adhesive pads on the skin.

Despite these influential factors, the implemented control via a shoulder position sensor results in a good balance between false negative (negligible) and true positive command detection. Further on, the fast configuration allows the user to easily adapt the parameters of the control when the performance decreases over time.

4.4 EEG-Study – Data Analysis

Cross validation results show the potential to control the neuroprosthesis in a 2-class scenario with 2 different movements of the same upper limb with EEG. All participants were at some timepoint above their significance threshold and overall a mean accuracy of 66,25 % was calculated, with the highest at 70,69 % and the lowest at 60,31 %. The best classification point is always between 0,9 and 2 s after the movement onset with a mean at 1,48 s. This means that the highest discriminability of the time domain signal is in the range started at the movement onset to 2 s thereafter, since the features are always constructed from a one second window before the best classification timepoint. Consider a reaction time of about 300 ms, this observation coincides with given literature of different MRCP components [52], where the most distinguishable signal in the movement versus movement case occurs around the movement onset [37]. Despite two participants have shown a high amount of artefacts included in the data (EH2, Ei9), in Table 5 one can see that for the other participants and their cross validated time classification analysis (Figure 17-Figure 27) comparable patterns and results could be observed. The difference in the classification timepoints might be explainable by the different reaction times and the different interpretations of the paradigm. The paradigm design introduces variations for the movement onset between participants, since they were instructed that not the exact synchronization with the paradigm is important but the constant execution and timing of the movement during the whole procedure.

Also, it is observable that most participants were able to control the neuroprosthesis online above the significance level of about 58 % (100 trials, α=0.05, adjusted Wald interval). Only 3 participants show a lower accuracy for the feedback, whereas for one of those persons this low accuracy can be described with the high amount of artefacts. A maximum accuracy of 70 % and an average of 62 % was reached. When looking at the confusion matrices, no significant bias to one class is observable. By analyzing the classifier output over a specified time window, for example for DQ9 (see Figure 28), a defined pattern especially for the pronation class can be seen. For EH8 (see Figure 32) the same result for the palmar class is

visible. It can also occur that the classifier recognizes a pattern, but this pattern is similarly reflected in both movements, which means that the classifier could distinguish the 2 movements theoretically against the rest, but against each other, they are not well distinguishable (see Figure 30). Another important property becomes visible through this representation - the correct classification time. If the timing from training to testing varies, no further correct classification can be ensured. The idea of smoothing the classifier output to reduce the impact of inexact timing and also the impact of short-time classifier variations, improved the classification to a maximum of 77 % for participant EI8. Unfortunately, in average the classification accuracy could only be improved to a maximum of about 1,46 % by smoothing the output of 7 classifications (classifier output at the best classification timepoint smoothed with ±3 samples). A very good example of the positive effect of this classification output smoothing can be seen in the data of EJ4. Without further data processing, only a completely random classification seems to be possible, but on closer inspection a pattern for each class can be seen (Figure 26 and Figure 37). Consequently, the average method can increase the accuracy to 68% (improvement 17 %) by smoothing with ±7 samples. Already with ±3 samples, in average the best result, the classification accuracy reaches 65 %. This means it has improved from total random classification to a significant value.

The additionally analyzed movement versus rest condition (see Figure 42 and Table 7) showed high true positive rates (TPR) for detecting a rest trial up to a maximum of 95,93 % and an average of 83,74 %. Overall accuracy of the classification reached a maximum of 93,6 % and an average of 81,95 %. It is noticeable that the best classification timepoint is comparable to the best classification timepoint of the movement versus movement condition. The small bias to the rest condition is explainable by the usage of an unbalanced classifier and is intentional, since in a real scenario it is recommended to have at best no false positive movement classifications and tolerate false negative ones. Anyway, this additional analysis is only done offline and for the given cue-based scenario and therefore cannot be translated directly to real life usage.

A good description how the paradigm effects the measured signal can be identified in the grand average over all participants (Figure 39). The high peak at approximately 1.9 seconds before the movement onset is initiated by a response to the visual cue [53]. To eliminate the

effect of this visual evoked potential the time between the first appearance of the cue and the movement onset must be at least 2.5 s, otherwise the influence of this potential would be too high and overlap the MRCP.

At second 0, where the movement onset is initialized on the screen, plus a short delay the potential reaches its maximum negativity. This additional delay is due to the system and the reaction time of the individuals. Already, approximately 1 s before this maximum negativity, the negative shift starts. Within this period, the early and late phase of the "Bereitschaftspotential" is observable. Afterwards, the potential starts to swing back to its base level [52] [54]. The most discriminative part is given approximately when the potential arises to its maximum negativity.

Another aspect is visualized in Figure 40. Approximately around the electrode C1, the negative amplitude of the MRCP reaches its maximum. The movement was done with the right hand, which coincide with the lateralization of this type of brain signal. Furthermore, this electrode region is located above the primary motor cortex, and therefore, it can be assumed that this signal is really an MRCP and not caused from artifacts. Going more to the outer range of the electrodes the MRCP pattern becomes smaller and more blurred.

It turned out that the training has a big influence on the classification. As seven out of eleven participants were naive to BCI, means they had no previous experience with this type of studies, the right timing and behavior slowly stabilized during the study. A high increase of signal quality and MRCP pattern during the experiment is detectable. For example, in Figure 41, the data of EI8 for the measurement runs and the feedback runs is compared. During the first few measurements runs, the person had to train the timing and focus and therefore, the signal quality is worse than for the feedback runs, where already a good constant procedure was given. This effect is already visible after two measurement runs. The negativity of the MRCP reaches a higher maximum and the general structure of the MRCP gets sharper. This leads to the implication that it is possible to reach higher classification accuracies and better signal quality by increasing the training beforehand. But, for example for GRZ003, who is non-naive and had a lot of experience, especially recently to this study, the MRCP pattern of this measurement was worse than in previous studies. By visual inspection of the raw signal and the observation of the behavior during the experiment this was due to a lack of concentration and focus. To draw a conclusion, one of the most important parts to observe

discriminable patterns in MRCP measurements is to repeatedly point out the importance of high concentration to the paradigm and the task. This observation of ups and downs after extensive training is consistent with existing results from previous studies [55].

4.5 Future Improvements

Of course, this is a first approach of simplification for a modular build which is able to process a neuroprosthesis control and therefore, future improvements are necessary.

Another aspect to work on must be the EEG-signal quality. MRCP signals are quite small and very prone to artefacts and therefore, the water-based solution is currently not efficient enough for classification purposes. A possibility to keep the mobility aspect would be to use a gel-based wireless EEG-measurement system. Additionally, an aspect to work on are the selected features. In this case, only time-domain features of a predefined window were taken. These results in a relative high number of features, whereas only a fraction of them really contain relevant information and this led to a lower classification performance. A way to counteract this unnecessarily high feature size is, to not only observe the time domain features but combine them with spectral features and afterwards perform a feature reduction method like principal component analysis to reduce the feature dimension [56].

Future analysis should focus more on the movement versus rest case in an online scenario. Therefore, it would be necessary to create a self-paced paradigm to remove the influence of the cues and commands and allow further conclusions about the ability of classifying in a more realistic scenario.

To improve the grasp patterns, the stimulation of agonist and antagonist muscles needs to be considered. When stimulating both muscle groups, the pattern might result in a more realistic grasp and it probably enables the improvement of the analog grasp control. Also, other default control methods, like EMG-based control, have to be added to widen the range of modularity and simplification for further usage in studies.

5. Conclusion

The EEG-study has shown that a discrimination of two movements or movement versus rest based on low frequency time domain signals of a neuroprosthesis or other similar devices is theoretically possible, even though the classification accuracy is not yet high enough to use it to control a neuroprosthesis for activities of daily living. In order to include this field of application, control by means of shoulder movements was successfully implemented. Anyway, implementing an environment which eases the usage of the FES-device in MATLAB/Simulink enables researchers to focus on other concept parts for further studies and provide an easily accessible structure for students to work within the area of functional electrical stimulation. This means that the implemented environment is a good starting point for future research to finally reach the goal of increasing the autonomy of people with SCI by artificially control body parts.

Bibliography

[1] C. R. Anderson, K. W. Ashwell, H. Collewijn, A. Conta, A. Harvey, C. Heise, S. Hodgetts, G. Holstege, G. Kayalioglu, J. R. Keast, S. McHanwell, E. M. McLachlan, G. Paxinos, G. Plant, O. Scremin, A. Sidhu, D. Stelzner and C. Watson, The Spinal Cord, Academic Press, 2009.

[2] M. J. Aminoff, F. Boller and D. F. Swaab, Handbook of Clinical Neurology, Elsevier B.V., 2012.

[3] A. M. Bryden, A. E. Peljovich , H. A. Hoyen, G. Nemunaitis, K. L. Kilgore and M. W. Keith, "Surgical restoration of arm and hand function in people with tetraplegia," *Topics in spinal cord injury rehabilitation,* vol. 18(1), pp. 43-49, 2012.

[4] G. Snoek, M. Ijzerman, H. Hermens, D. Maxwell and F. Biering-Sorensen, "Survey of the needs of patients with spinal cord injury: impact and priority for improvement in hand function in tetraplegics," *Spinal Cord,* vol. 42, pp. 526-532, 2004.

[5] C. Hammond, "Neurons," in *Cellular and Molecular Neurophysiology*, Academic Press, 2015, pp. 3-23.

[6] G. Shroff, D. Thakur, V. Dhingra, D. Singh Baroli, D. Khatri and R. Dev Gautam, "Role of physiotherapy in the mobilization of patients with spinal cord injury undergoing human embryonic stem cells transplantation," *Clinical and Translational Medicine,* vol. 5, 2016.

[7] J. M. Schwab, K. Brechtel, C.-A. Mueller, V. Failli, H.-P. Kaps, S. K. Tuli and H. J. Schluesener, "Experimental strategies to promote spinal cord regeneration-an integrative perspective," *Progress in Neurobiology ,* vol. 78, pp. 91-116, 2006.

[8] M. W. Keith and A. Peljovich, "Chapter 10 - Surgical treatments to restore function control in spinal cord injury," in *Handbook of Clinical Neurology*, Elsevier, 2012, pp. 167-179.

[9] W. Pschyrembel and U. Arnold, Pschyrembel Klinisches Wörterbuch, De Gruyter, 2014.

[10] K.-P. Hoffmann , M. C. Carrozza, S. Micera and K. Koch, "Neuroprothesen - Implantierbare Mikrosysteme auf der Grundlage von Methoden der Neurobionik," in *Orthopädie-Technik*, 2006, pp. 334-339.

[11] W. Platzer, H. Fritsch, W. Kahle and G. Spitzer, Taschenatlas der Anatomie - Bewegungsapparat, Stuttgart: Thieme, 2009.

[12] C. A. Greig and D. A. Jones, "Muscle physiology and contraction," *Surgery,* vol. 34, no. 3, pp. 107-114, 2016.

[13] G. G. Matthews, "Neural Control of Muscle Contraction," in *Cellular Physiology of Nerve and Muscle*, Blackwell Science Ltd, 2003, pp. 177-187.

[14] S. Salmons, "Skeletal Muscle," in *Neuroprosthetics - Theory and Practice*, Utah, USA, World Scientific Publishing Co. Pte. Ltd, 2004, pp. 158-183.

[15] M. R. Popovic and A. T. Thrasher, "Neuroprostheses," in *Encyclopedia of Biomaterials and Biomedical Engineering*, New York, Marcel Dekker, Inc., 2004, pp. 1056-1065.

[16] T. Keller and A. Kuhn, "Electrodes for transcutaneous (surface) electrical stimulation," *Journal of Atomatic Control,* vol. 18, no. 2, pp. 35-45, 2008.

[17] L. A. Geddes and J. D. Bourland, "The Strength-Duration Curve," *IEEE transactions on bio-medical engineering,* vol. 32, no. 6, pp. 458-459, 1985.

[18] I. Mogyoros, M. C. Kiernan and D. Burke, "Strength-duration properties of human peripheral nerve," *Brain,* vol. 119, pp. 439-447, 1996.

[19] J. Claßen and A. Schnitzler, Interventionelle Neurophysiologie: Grundlagen und therapeutische Anwendungen, Stuttgart: Georg Thieme Verlag KG, 2013.

[20] H. P. Peckham and J. S. Knutson, "Functional Electrical Stimulation for Neuromuscular Applications," *Annual Review of Biomedical Engineering,* vol. 7, pp. 327-360, 2005.

[21] M. Lawrence, G.-P. Gross, M. Lang, A. Kuhn , T. Keller and M. Morari, "Assessment of Finger Forces and Wrist Torques for Functional Grasp Using New Multichannel Textile Neuroprostheses," *Artificial Organs,* pp. 32(8):634-638, 2008.

[22] Y. Hara, "Neurorehabilitation with New Functional Electrical Stimulation for Hemiparetic Upper Extremity in Stroke Patients," *Journal of Nippon Medical School,* pp. 75(1): 4-14, 2008.

[23] M. Rohm, M. Schneiders, C. Müller, A. Kreilinger , V. Kaiser, G. R. Müller-Putz and R. Rupp, "Hybrid brain–computer interfaces and hybrid neuroprostheses for restoration of upper limb functions in individuals with high-level spinal cord injury," *Artificial Intelligence in Medicine,* pp. 59: 133-142, 2013.

[24] J. d. R. Millán, R. Rupp, G. R. Müller-Putz, R. Murray-Smith, C. Giugliemma, M. Tangermann, C. Vidaurre, F. Cincotti, A. Kübler, R. Leeb, C. Neuper, K. R. Müller and D. Mattia, "Combining brain-computer interfaces and assistive technologies: state-of-the-art and challenges," *frontiers in Neuroscience,* vol. 4, no. 161, pp. 1-15, 2010.

[25] J. R. Wolpaw, N. Birbaumer, D. J. McFarland, G. Pfurtscheller and T. M. Vaughan, "Brain–computer interfaces for communication and control," *Clinical Neurophysiology,* vol. 113, pp. 767-791, 2002.

[26] D. B. Popovic and T. Sinkjær, "Central nervous System Lesions Leading to Disability," *JOURNAL OF AUTOMATIC CONTROL,* vol. 18, no. 2, pp. 11-23, 2008.

[27] J. Feher, "4.5 - Balance and Control of Movement," in *Quantitative Human Physiology*, Boston, Academic Press, 2012, pp. 341-353.

[28] R. A. Ramadan and A. V. Vasilakos, "Brain computer interface: control signals review," *Neurocomputing,* vol. 223, pp. 26-44, 2017.

[29] D. J. McFarland and J. R. Wolpaw, "Brain-computer interfaces for communication and control," *Commun. ACM,* vol. 54, no. 5, p. 60, 2011.

[30] G. Müller-Putz, R. Scherer, G. Pfurtscheller and R. Rüdiger, "Brain-computer interfaces for control of neuroprostheses: from synchronous to asynchronous mode of operation / Brain-Computer Interfaces zur Steuerung von Neuroprothesen: von der synchronen zur asynchronen Funktionsweise," *Biomedizinische Technik/Biomedical Engineering,* vol. 51, no. 2, pp. 57-63, 2006.

[31] G. Pfurtscheller, C. Guger, G. Müller, G. Krausz and C. Neuper, "Brain oscillations control hand orthosis in a tetraplegic," *Neuroscience Letters,* no. 292, pp. 211-214, 2000.

[32] G. Pfurtscheller, G. Müller-Putz, J. Pfurtscheller and R. Rupp, "EEG-Based Asynchronous BCI Controls Functional Electrical Stimulation in a Tetraplegic Patient," *EURASIP J. Adv. Signal Process.,* vol. 2005, no. 19, 2005.

[33] A. Kreilinger, V. Kaiser, M. Rohm, R. Rupp and G. Müller-Putz, "BCI and FES Training of a Spinal Cord Injured End-User to Control a Neuroprosthesis," *Biomed. Tech. ,* 2013.

[34] T. Pistohl, A. Schulze-Bonhage, A. Aertsen, C. Mehring and T. Ball, "Decoding natural grasp types from human ECoG," *Neuroimage,* vol. 59, no. 1, pp. 248-260, 2012.

[35] H. Shibasaki and M. Hallett, "What is the Bereitschaftspotential?," *Clinical Neurophysiology,* vol. 117, pp. 2341-2356, 2006.

[36] M. Jochumsen, I. K. Niazi, D. Taylor, D. Farina and K. Dremstrup, "Detecting and classifying movement-related cortical potentials associated with hand movements in healthy subjects and stroke patients from single-electrode, single-trial EEG," *Journal of neural engineering,* vol. 12, no. 5, 2015.

[37] P. Ofner , A. Schwarz, J. Pereira and G. Müller-Putz, "Upper limb movements can be decoded from the time-domain of low-frequency EEG," *PLOS ONE,* vol. 12, no. 8, p. e0182578, 2017.

[38] R. Rupp, A. Kreilinger, M. Rohm, V. Kaiser and G. R. Müller-Putz, "Development of a non-invasive, multifunctional grasp neuroprosthesis and its evaluation in an individual with a high spinal cord injury," in *34th Annual Internatiol Conference of the IEEE EMBS*, San Diego, California USA, 2012.

[39] R. Putz and R. Pabst, Sobotta - Atlas of Human Anatomy, vol. Volume 1, München: Elsevier GmbH, 2006.

[40] "tools4bci," Institute for Knowledge Discovery, Graz University of Technology, Chair in Non-invasive Brain-machine Interface at EPFL, [Online]. Available: http://tools4bci.sourceforge.net/. [Accessed 19 12 2018].

[41] G. R. Müller-Putz, C. Breitwieser, F. Cincotti, R. Leeb, M. Schreuder, F. Leotta, M. Tavella, L. Bianchi, A. Kreilinger, A. Ramsay, M. Rohm, M. Sagebaum, L. Tonin, C. Neuper and J. d. R. Millan, "Tools for Brain-Computer Interaction: A General Concept for a Hybrid BCI," *Frontiers in neuroinformatics,* vol. 5, no. 30, pp. 1-10, 2011.

[42] "biosig," TU Graz, IST Austria, [Online]. Available: http://biosig.sourceforge.net/. [Accessed 19 12 2018].

[43] A. Delorme and S. Makeig, "EEGLAB: an open source toolbox for analysis of single-trial EEG dynamics including independent component analysis," *Journal of Neuroscience Methods,* vol. 134, no. 1, pp. 9-21, 2004.

[44] A. Schwarz, P. Ofner , J. Pereira , A. I. Sburlea and G. R. Müller-Putz, "Decoding natural reach-and-grasp actions from," *Journal of Neural Engineering,* vol. 15, no. 016005, pp. 1-14, 2018.

[45] C. M. Bishop, "4. Linear Models for Classification - 4.1 Discriminant Functions," in *Pattern Recognition and Machine Learning*, New York, Springer Science+Business Media, 2006, pp. 179-192.

[46] B. Blankertz, S. Lemm, M. Treder, S. Haufe and K.-R. Müller, "Single-trial analysis and classification of ERP components — A tutorial," *NeuroImage,* vol. 56, no. 2, pp. 814-825, 2011.

[47] G. R. Müller-Putz, R. Scherer, C. Brunner, R. Leeb and G. Pfurtscheller, "Better than random? A closer look on BCI results," *International Journal of Bioelectromagnetism,* vol. 10, no. 1, pp. 52-55, 2008.

[48] M. Billinger, I. Daly, V. Kaiser, J. Jin, B. Allison, G. R. Müller-Putz and C. Brunner, "Is It Significant? Guidelines for Reporting BCI Performance," in *Towards Practical Brain-Computer Interfaces, Biological and Medical Physics, Biomedical Engineering*, Berlin-Heidelberg, Springer, 2012, pp. 333-354.

[49] J. Dien, "Issues in the application of the average reference: Review, critiques, and recommendations," *Behavior Research Methods, Instruments, & Computers,* vol. 30, no. 1, pp. 34-43, 1998.

[50] A. Pinegger, S. C. Wriessnegger, J. Faller and G. R. Müller-Putz, "Evaluation of Different EEG Acquisition Systems Concerning Their Suitability for Building a Brain-Computer Interface: Case Studies," *frontiers in Neuroscience,* vol. 10, no. 441, pp. 1-11, 2016.

[51] V. Mihajlovic, G. · Garcia Molina and J. Peuscher, "To what extent can dry and water-based EEG electrodes replace conductive gel ones?: A Steady State Visual Evoked Potential Brain-Computer Interface Case Study," in *ICBE 2011: International Conference on Biomedical Engineering*, Venice, Italy, 2011.

[52] A. Shakeel, M. S. Navid, M. N. Anwar, S. Mazhar, M. Jochumsen and I. K. Niazi, "A Review of Techniques for Detection of Movement Intention Using Movement-Related Cortical Potentials," *Computational and Mathematical Methods in Medicine,* vol. 2015, pp. 1-13, 2015.

[53] J. Elshout and G. G. Molina, "Review of Brain-Computer Interfaces based on the P300 evoked potential," Koninklijke Philips Electronics, 2009.

[54] P. Ashlesh and K. K. Preet, "Bereitschaftspotentials as a Tool to Study Motor Neuroscience," *International Journal of Science and Research (IJSR),* vol. 5, no. 12, pp. 1580-1587, 2016.

[55] M. Jochumsen, C. Rovsing, H. Rovsing, S. Cremoux, N. Signal, K. Allen, D. Taylor and I. K. Niazi, "Quantification of Movement-Related EEG Correlates Associated with Motor Training: A Study on Movement-Related Cortical Potentials and Sensorimotor Rhythms," *Frontiers in human neuroscience,* vol. 11, no. 604, pp. 1-11, 2017.

[56] M. Jochumsen, I. Niazi, K. Dremstrup and E. Kamavuako, "Detecting and classifying three different hand movement types through electroencephalography recordings for neurorehabilitation," *Medical & Biological Engineering & Computing,* vol. 54, p. 1491–1501, 2016.

[57] G. R. Müller-Putz, R. Scherer, G. Pfurtscheller and C. Neuper , "Temporal coding of brain patterns for direct limb control in humans," *Frontiers in Neuroscience,* vol. 4, no. 34, pp. 1-11, 2010.

List of figures

Appendix

In the first part of the appendix the detailed additional Simulink structures are shown. This includes the keyboard control, the measurement system as well as the feedback system without FES.

Further, the individual results are visualized. The MRCPs of every participant as well as the detailed performance evaluation of the movement versus rest condition is given. The processing was done in the same way as it is described in the methods.

The last part of the appendix includes a small step by step guide to configure the FES-device and use it within a Simulink model.

Simulink system structures

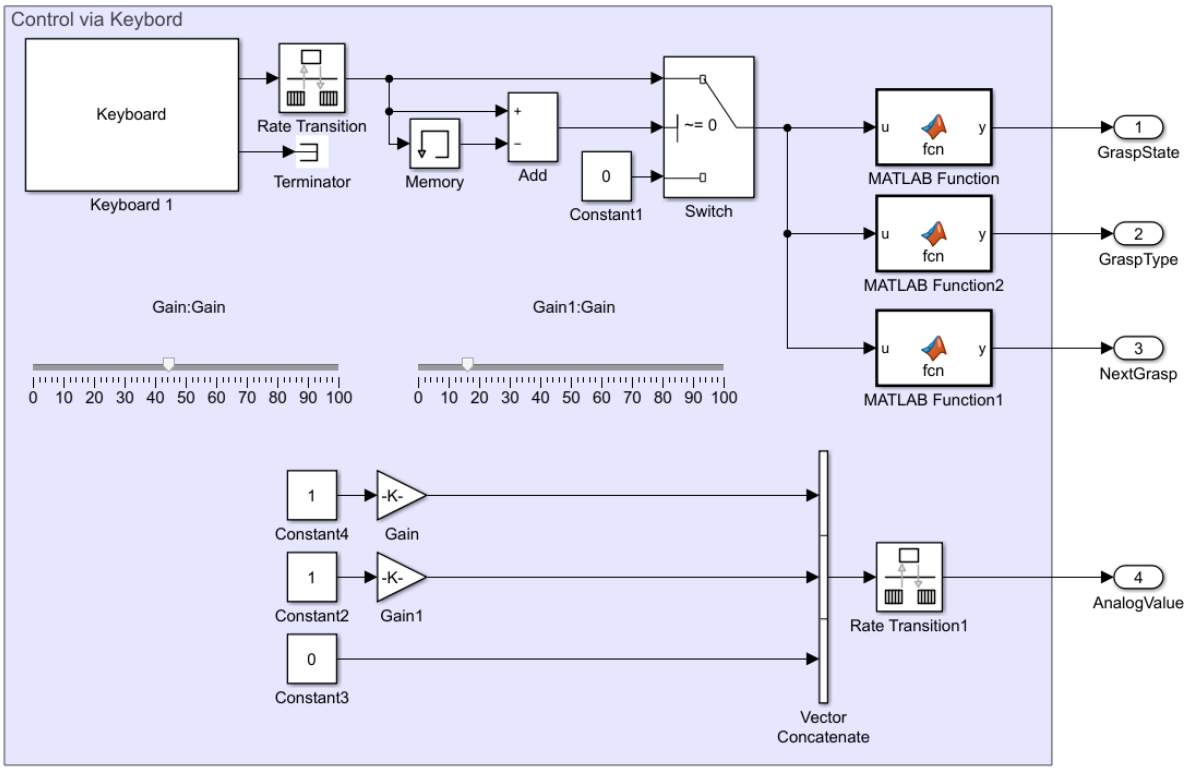

A.Figure 1: Simulink structure for keyboard control, output 16 Hz, control via defined keyboard inputs

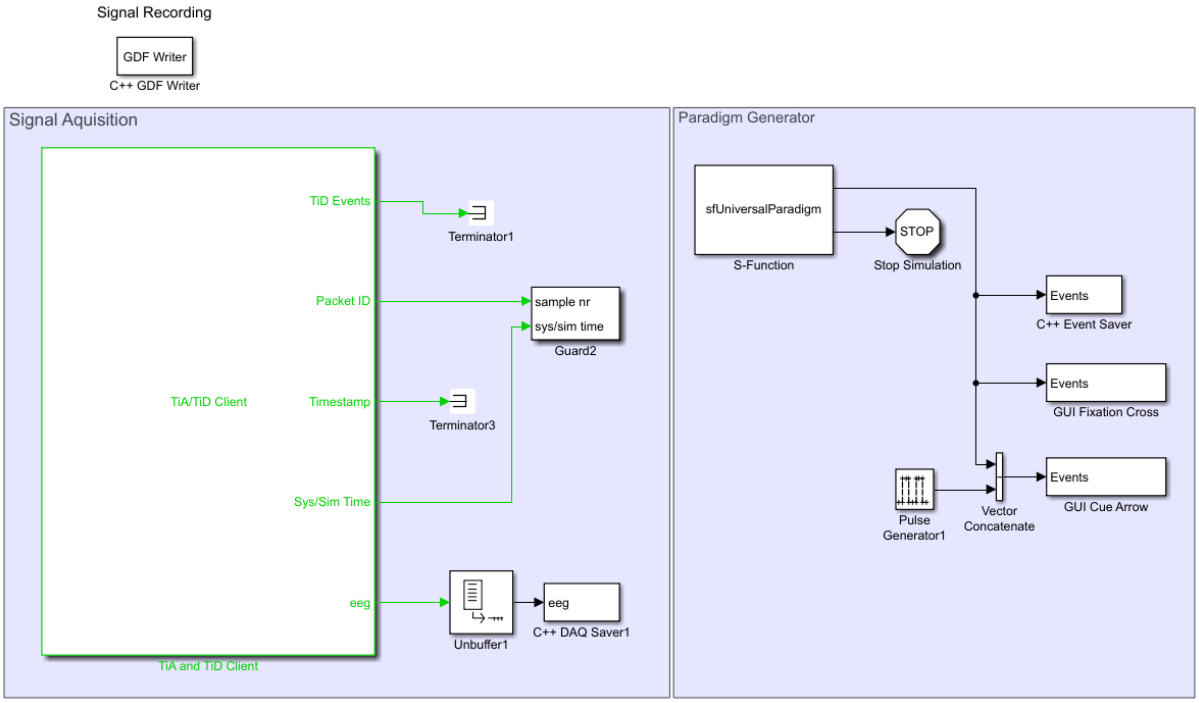

A.Figure 2: Simulink structure of the measurement system with signal acquisition and paradigm generation, sampling frequency: 256 Hz,

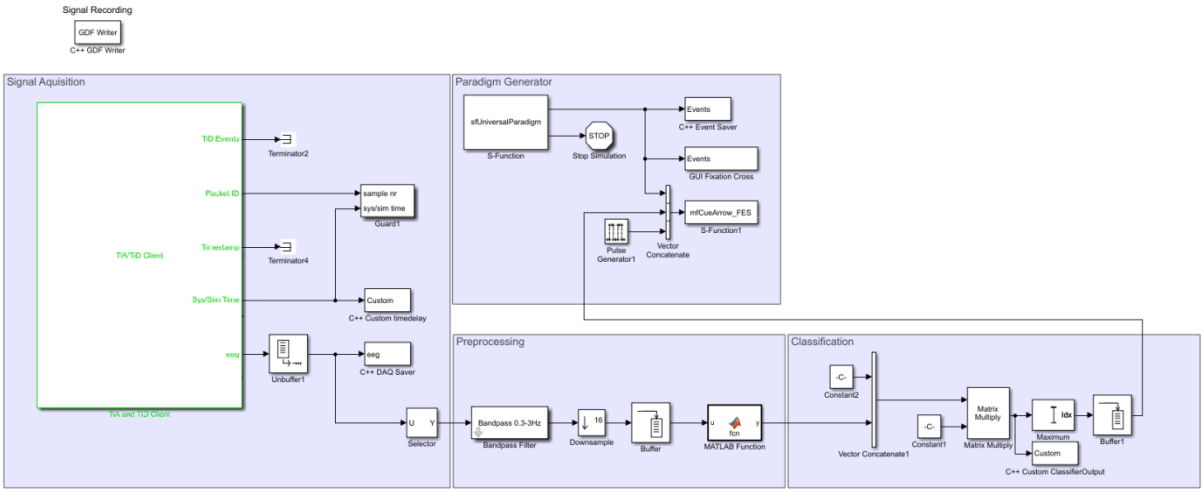

A.Figure 3: Simulink structure of the Feedback system without FES with signal acquisition, paradigm generation, preprocessing and classification block, sampling frequency: 256 Hz

MRCP Measurement Runs and Performance Evaluation (mov. vs. rest) of each participant

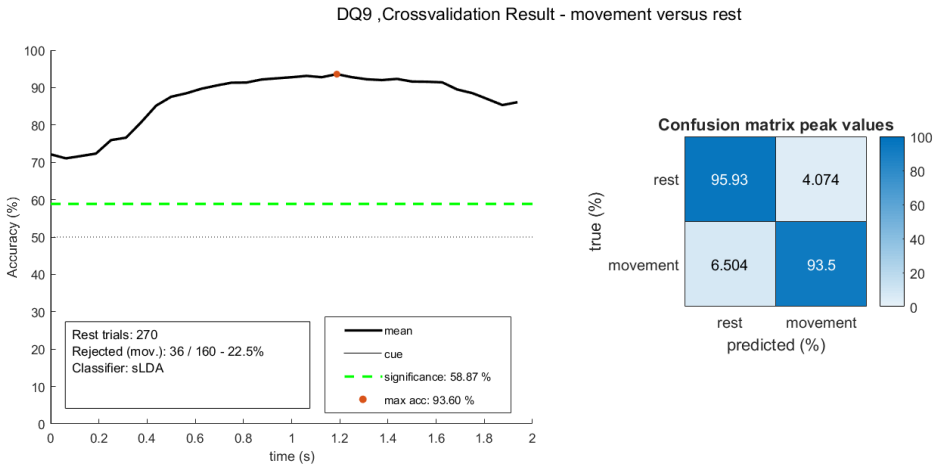

A.Figure 4: Participant DQ9 - Offline performance evaluation by cross-validation for movement versus rest condition, right side: truth table

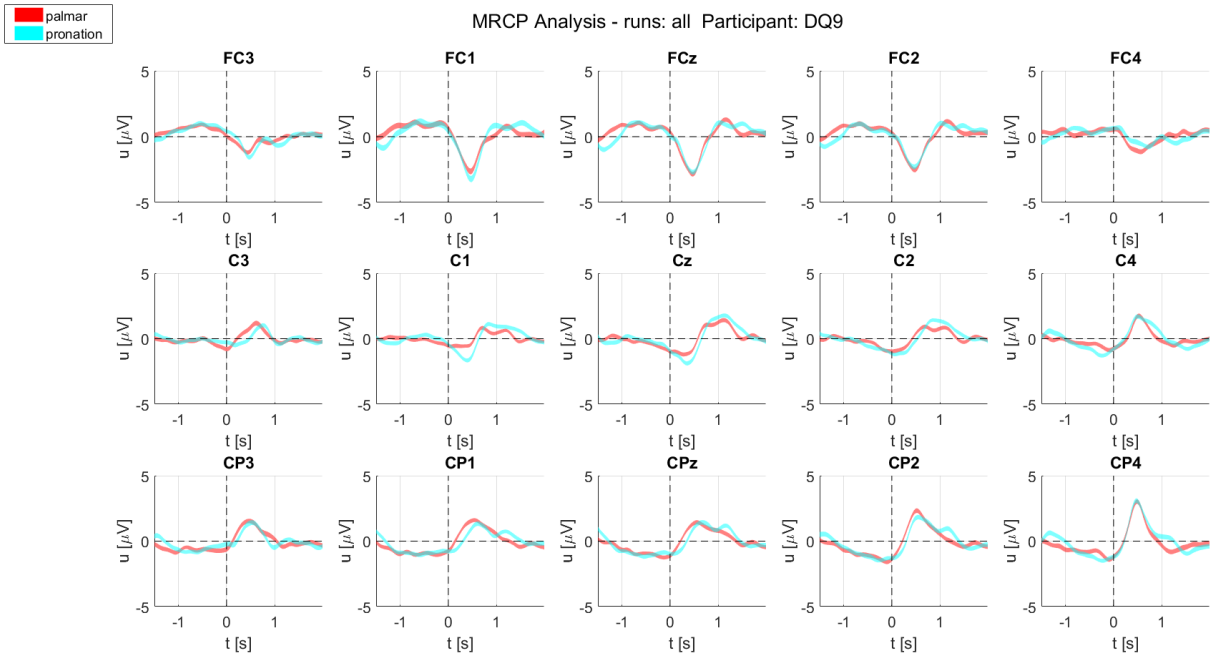

A.Figure 5: Participant DQ9 - MRCP Analysis for all runs, CAR filtered, time: -1.5 – 2 seconds around movement onset

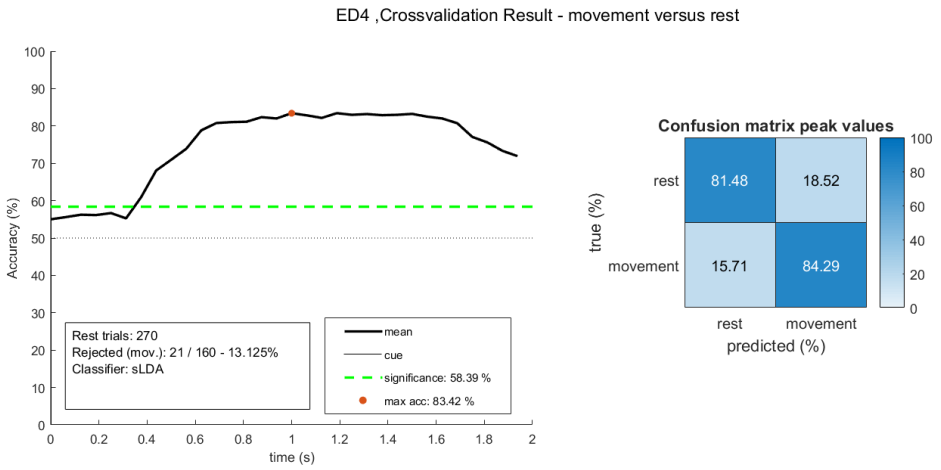

A.Figure 6: Participant ED4 - Offline performance evaluation by cross-validation for movement versus rest condition, right side: truth table

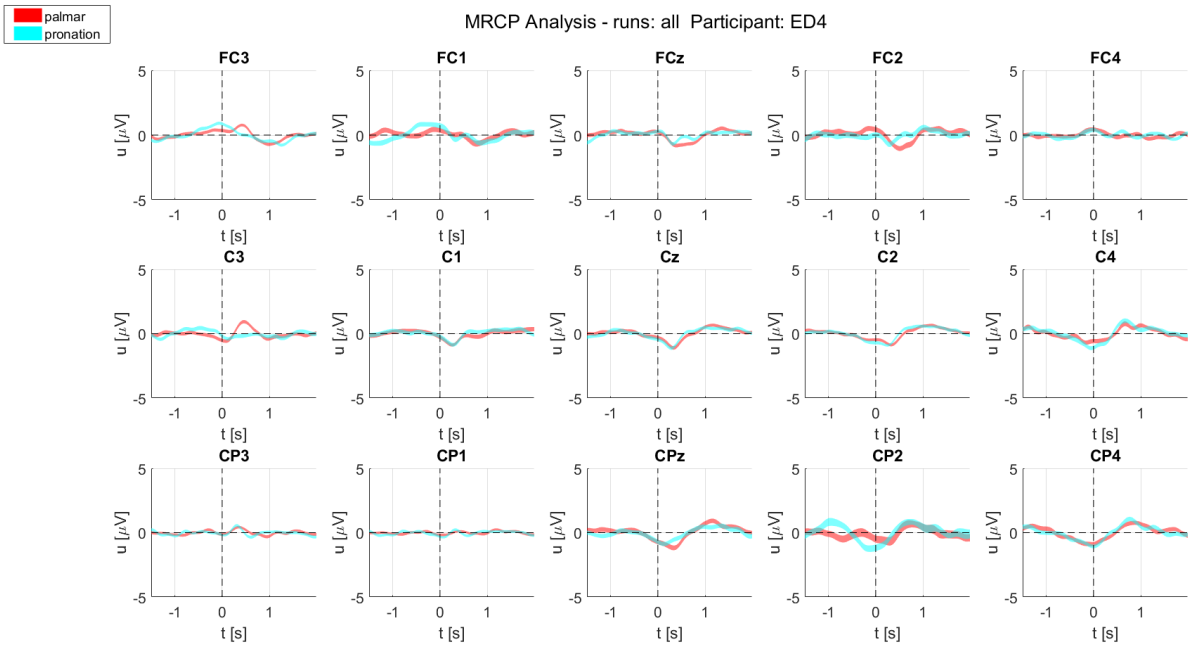

A.Figure 7: Participant ED4 - MRCP Analysis for all runs, CAR filtered, time: -1.5 – 2 seconds around movement onset

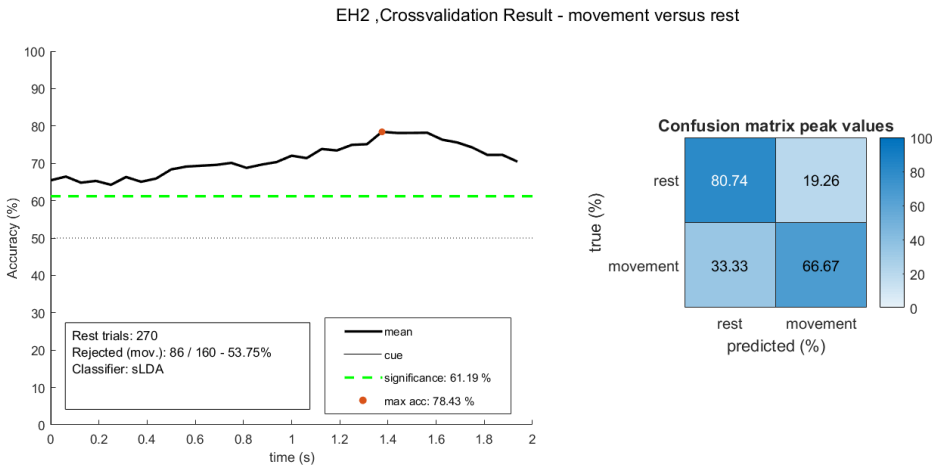

A.Figure 8: Participant EH2 - Offline performance evaluation by cross-validation for movement versus rest condition, right side: truth table

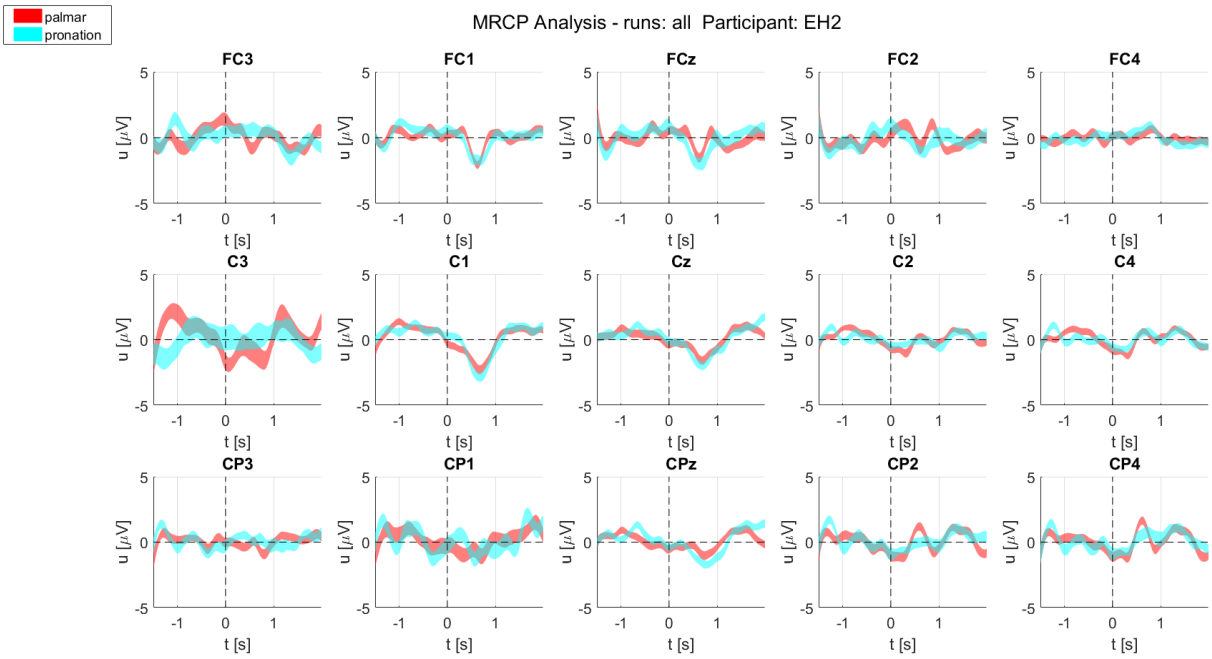

A.Figure 9: Participant EH2 - MRCP Analysis for all runs, CAR filtered, time: -1.5 – 2 seconds around movement onset

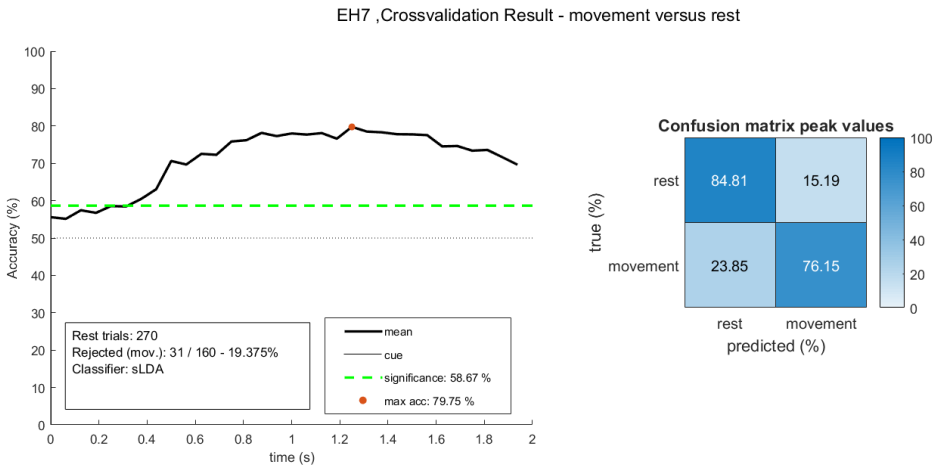

A.Figure 10: Participant EH7 - Offline performance evaluation by cross-validation for movement versus rest condition, right side: truth table

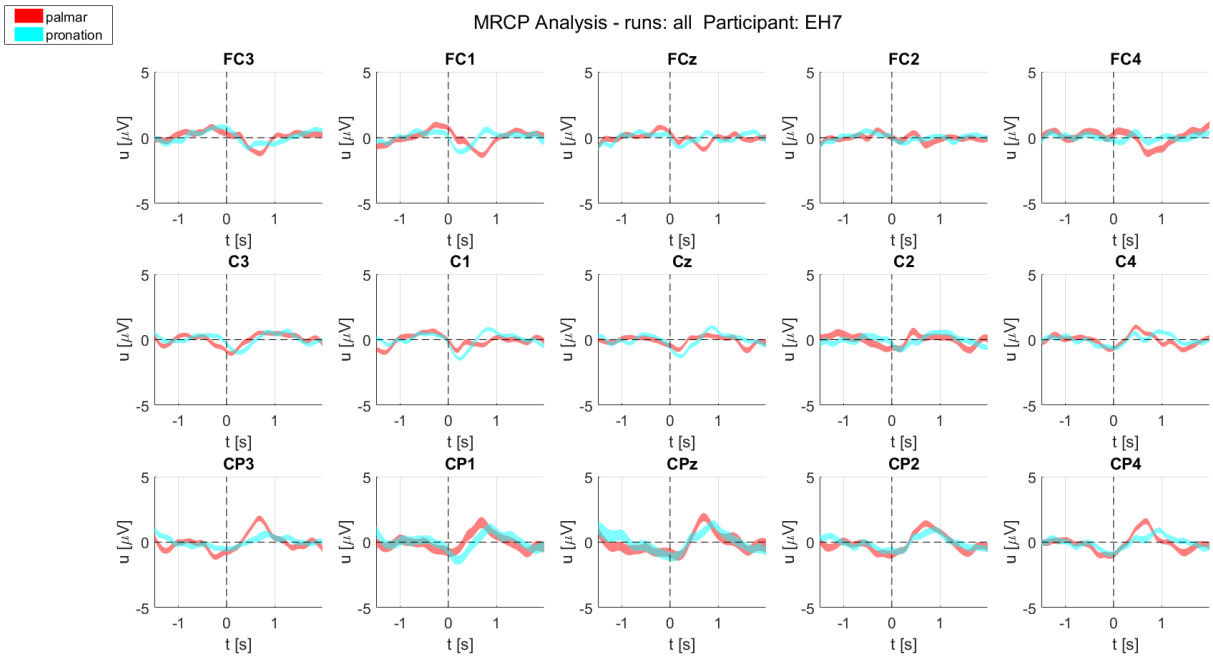

A.Figure 11: Participant EH7 - MRCP Analysis for all runs, CAR filtered, time: -1.5 – 2 seconds around movement onset

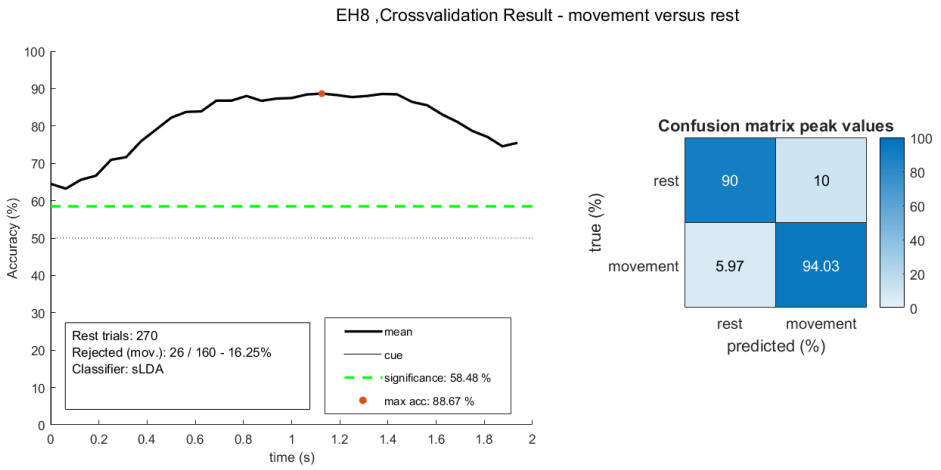

A.Figure 12: Participant EH8 - Offline performance evaluation by cross-validation for movement versus rest condition, right side: truth table

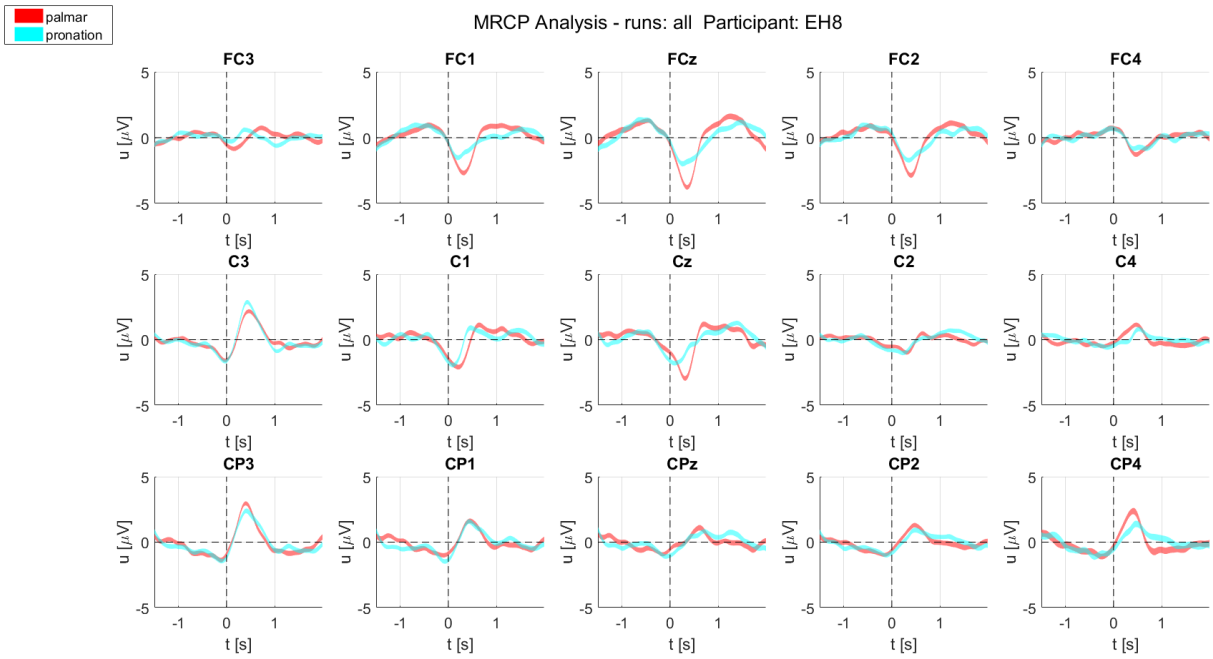

A.Figure 13: Participant EH8 - MRCP Analysis for all runs, CAR filtered, time: -1.5 – 2 seconds around movement onset

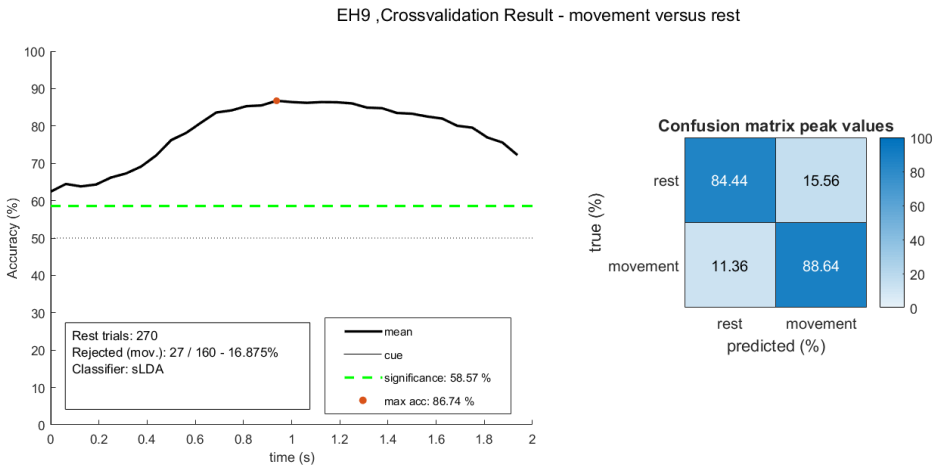

A.Figure 14: Participant EH9 - Offline performance evaluation by cross-validation for movement versus rest condition, right side: truth table

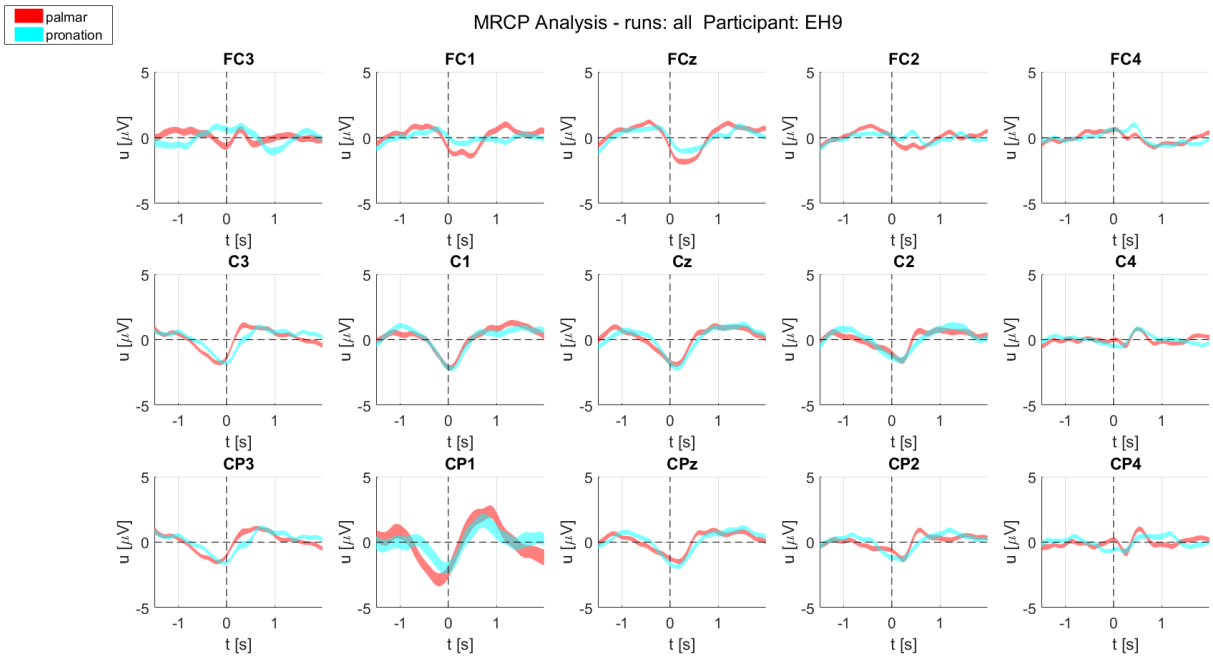

A.Figure 15: Participant EH9 - MRCP Analysis for all runs, CAR filtered, time: -1.5 – 2 seconds around movement onset

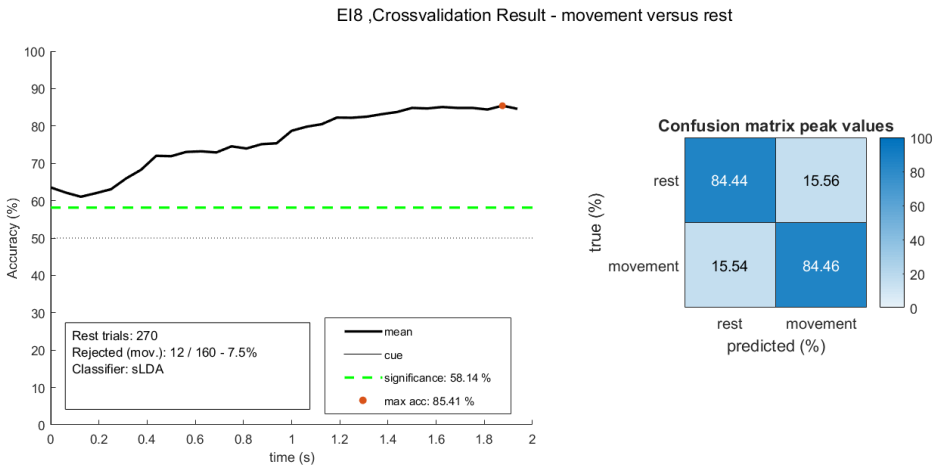

A.Figure 16: Participant EI8 - Offline performance evaluation by cross-validation for movement versus rest condition, right side: truth table

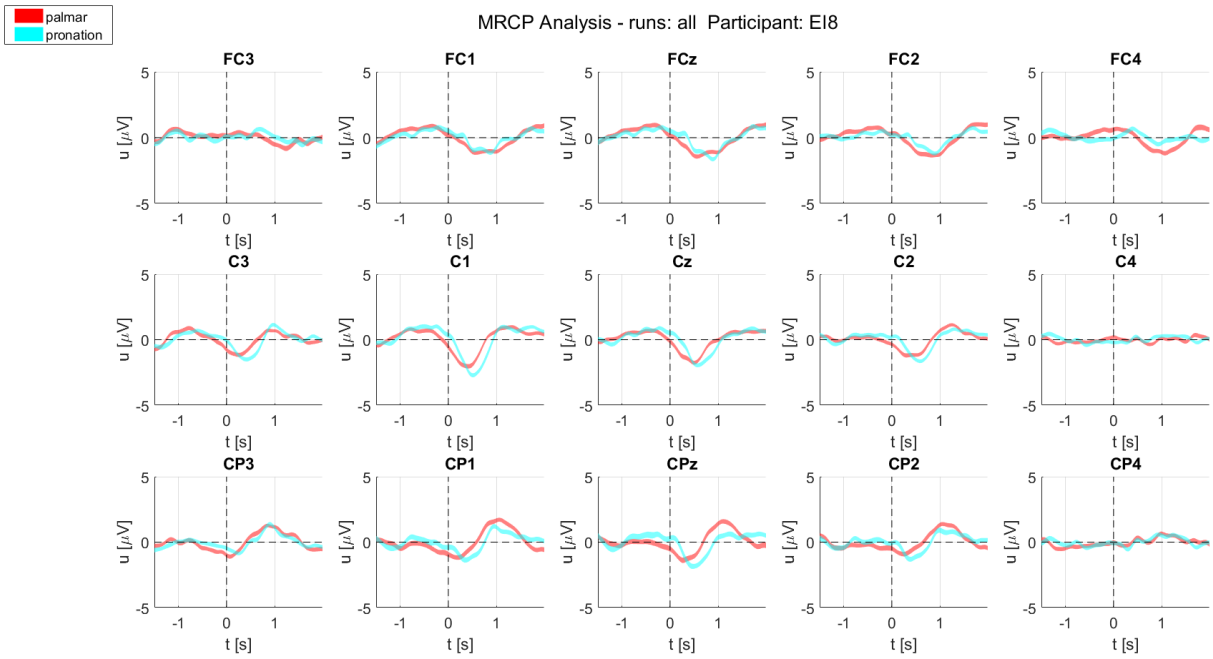

A.Figure 17: Participant EI8 - MRCP Analysis for all runs, CAR filtered, time: -1.5 – 2 seconds around movement onset

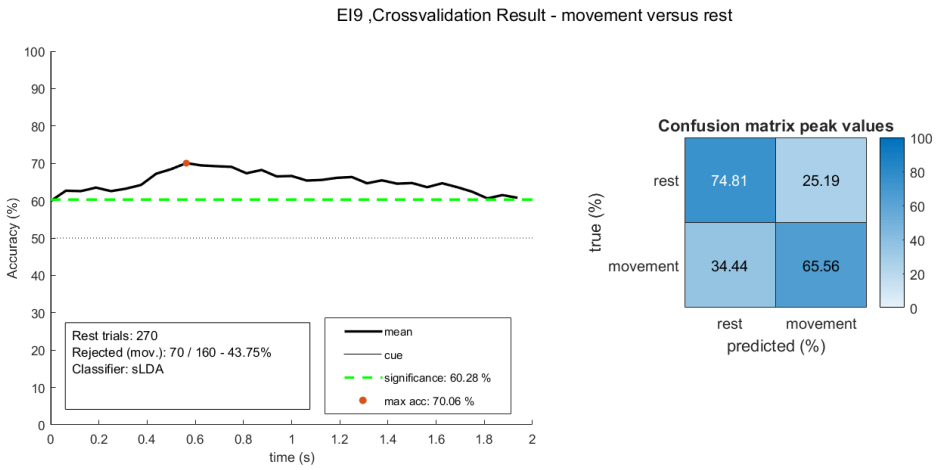

A.Figure 18: Participant EI9 - Offline performance evaluation by cross-validation for movement versus rest condition, right side: truth table

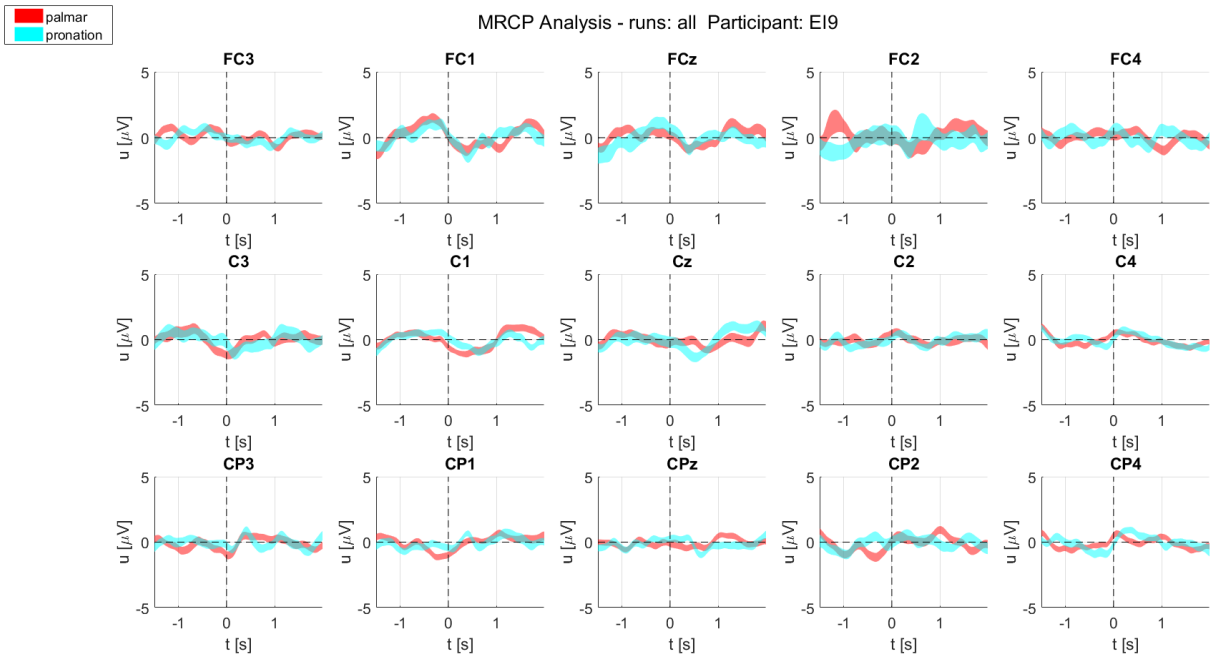

A.Figure 19: Participant EI9 - MRCP Analysis for all runs, CAR filtered, time: -1.5 – 2 seconds around movement onset

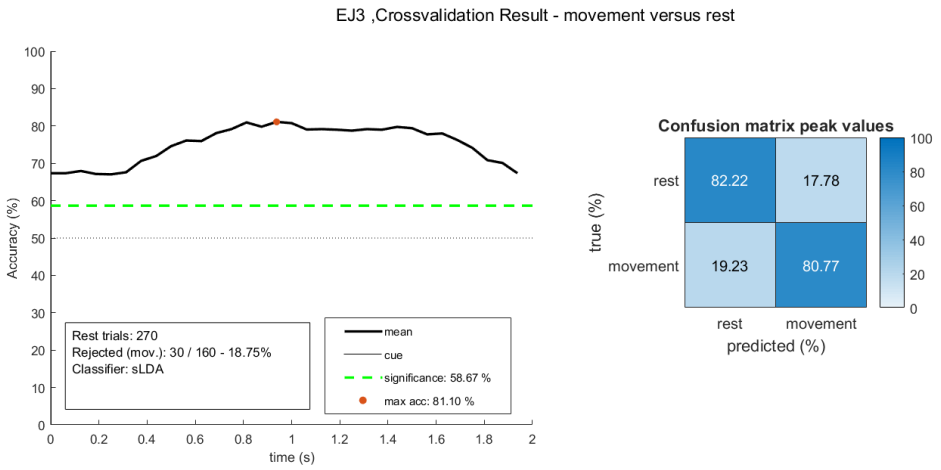

A.Figure 20: Participant EJ3 - Offline performance evaluation by cross-validation for movement versus rest condition, right side: truth table

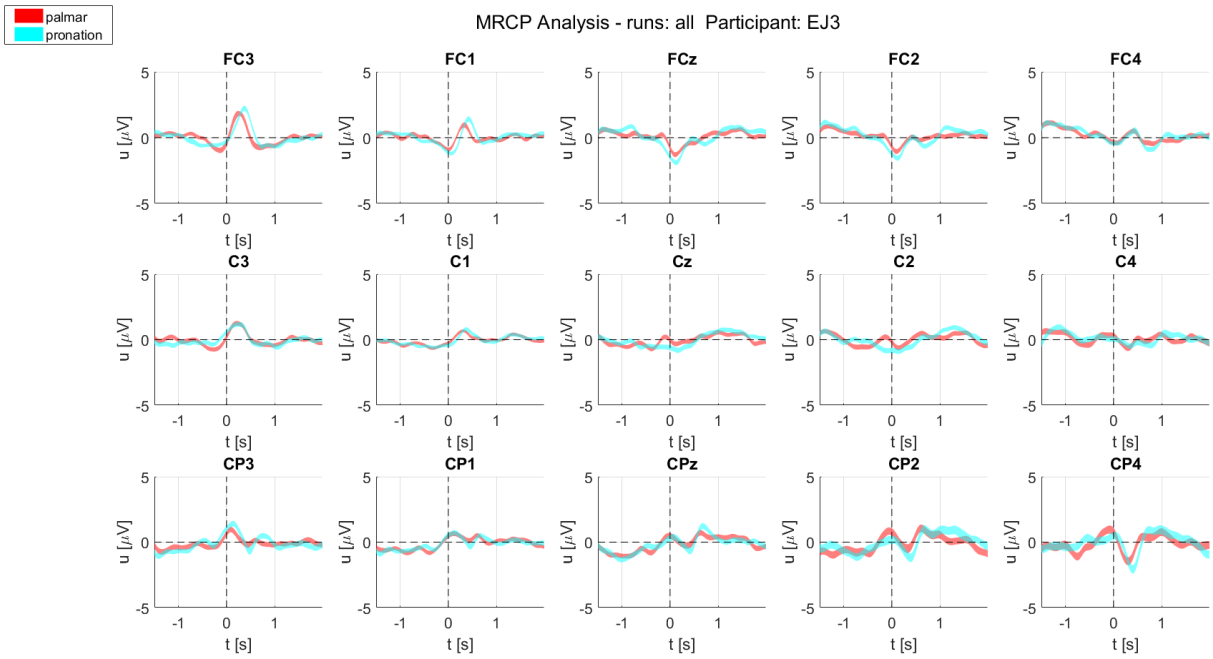

A.Figure 21: Participant EJ3 - MRCP Analysis for all runs, CAR filtered, time: -1.5 – 2 seconds around movement onset

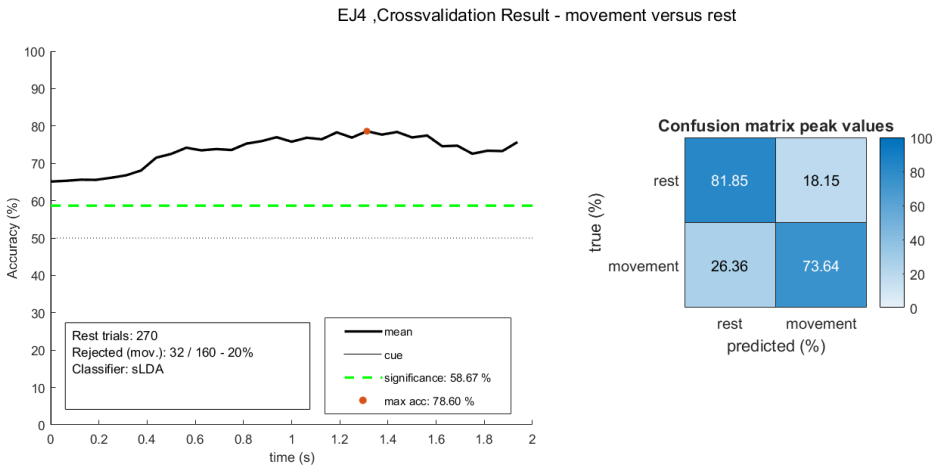

A.Figure 22: Participant EJ4 - Offline performance evaluation by cross-validation for movement versus rest condition, right side: truth table

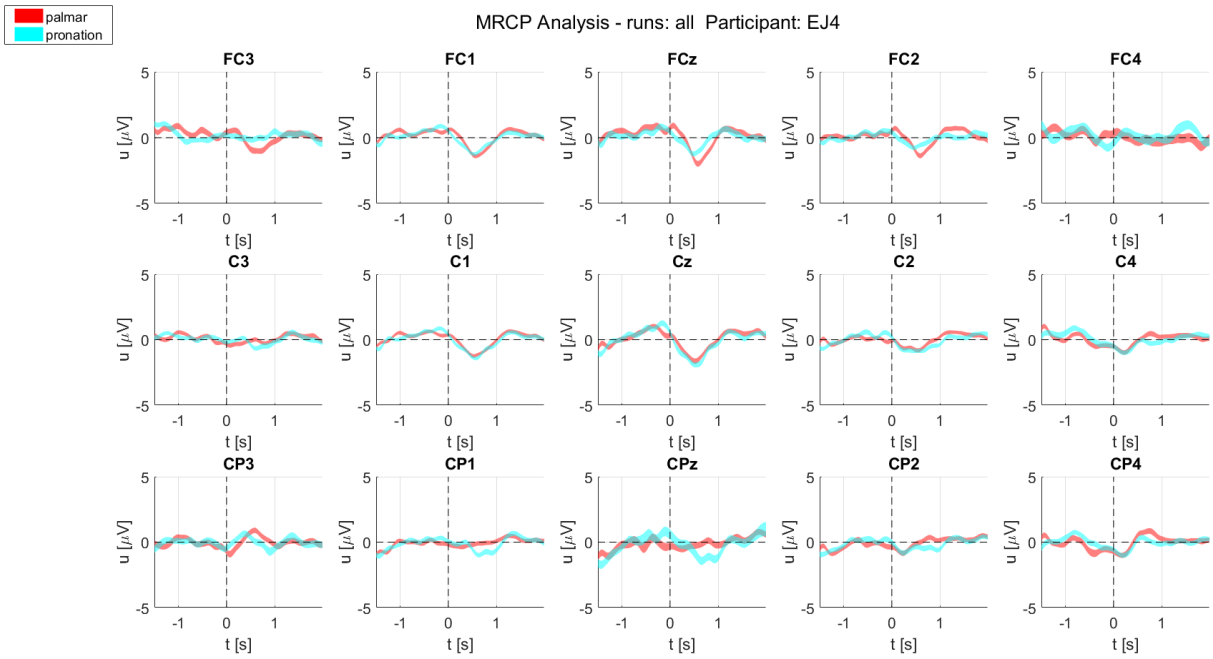

A.Figure 23: Participant EJ4 - MRCP Analysis for all runs, CAR filtered, time: -1.5 – 2 seconds around movement onset

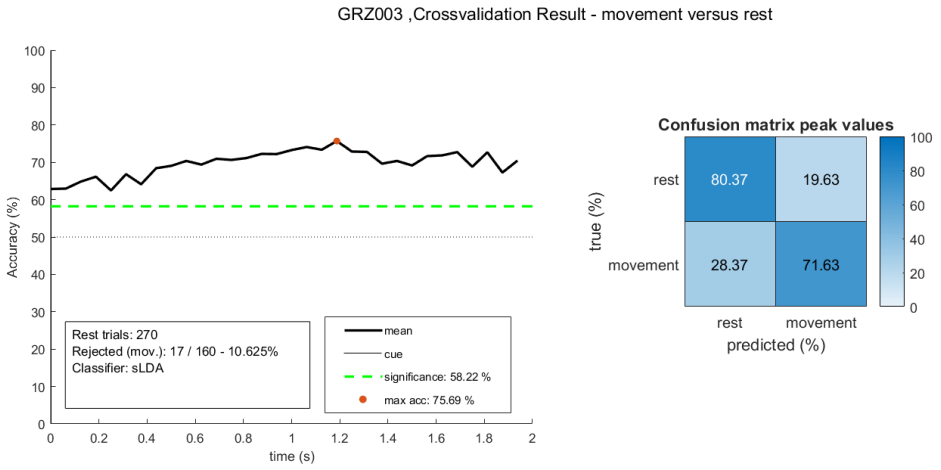

A.Figure 24: Participant GRZ003 - Offline performance evaluation by cross-validation for movement versus rest condition, right side: truth table

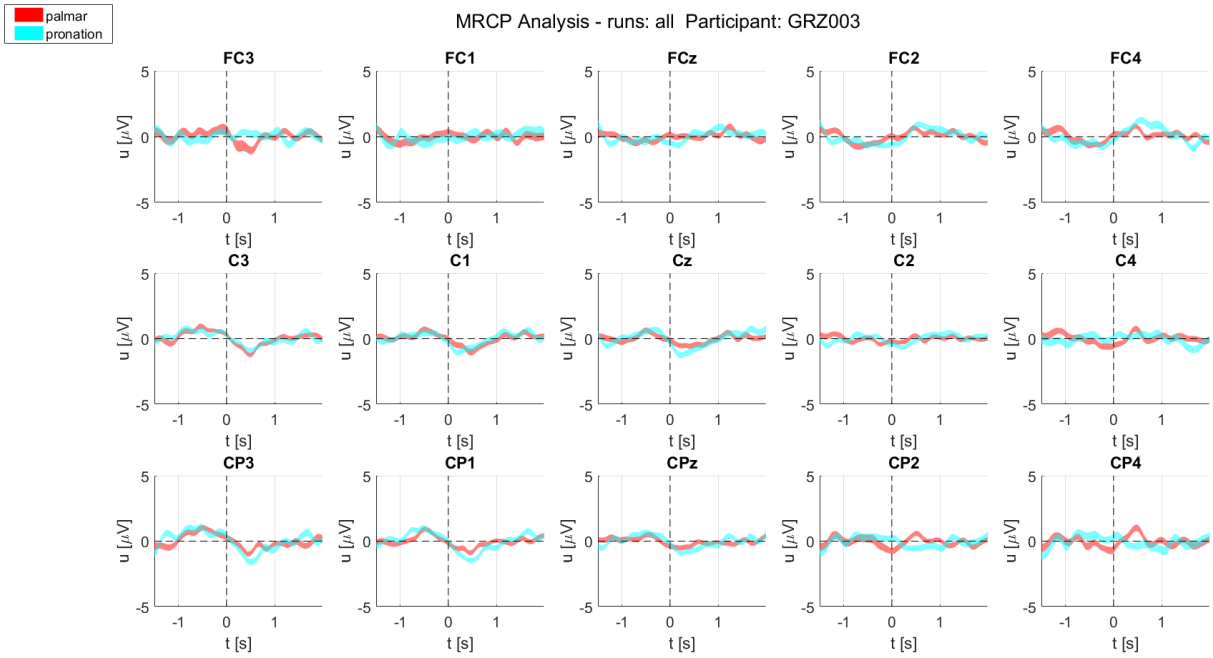

A.Figure 25: Participant GRZ003 - MRCP Analysis for all runs, CAR filtered, time: -1.5 – 2 seconds around movement onset

Step by step guide to configure the FES-device and create stimulations maps for neuroprosthesis control

First, it is necessary to copy the libraries correctly in your folder structure. Following structures and subfiles are required:

- lib/lib_FESMUX
- lib/lib_FESMUX_Config
- lib/lib_FESMUX_Control
- lib/general
- measurement_data/subject_master
- scripts/ConfigurationFES_JOY.m

Open the ConfigurationFES_JOY.m file in matlab →

Necessary adjustments:

- change subject name and information (line12/13)
- define FES-device (Motion Stim 8 with serial connection and optocoupling device or MG FESMUX-device with Bluetooth connection, both with latest Firmware from MG Project) and connect it to the CU.
- if MG FESMUX-device → add to coupled Bluetooth devices of operating system and change device name manually: lib/lib_FESMUX/getFESMuxConfig.m

If all is done correctly the configuration script can be started and the configuration can be made according to the visualized GUIs. Within this configuration it is necessary to place the according electrodes at the right positions and try to produce the correct wanted stimulation pattern. The “apply” button starts stimulation of the specified channel. If you need to change values change it by activating the “change startvalues” button. This seems to be a bit circumstantial, but it provides a save configuration environment which avoids involuntarily high stimulation amplitudes.

At the end, a new configuration file with the specified subject name is created, including the default map settings of palmar, lateral, pronation and the 3D map palmar/pronation. If you want to change the grasp maps or add more maps use the functions create_map and create_3Dmap. How to use them is described within the comments of the functions itself

and additionally the default maps provide good examples for usage. Keep care that the default figures (code lines 143 – 166) are made for the palmar, pronation and lateral map and therefore it is necessary to manually change them if grasp maps are changed.

First usage in Simulink:

After creating a configuration file, stimulation with Simulink can be done. Therefore, open the preloadscript_FES_block.m file with Matlab and, again, change the subject, hand, and FES-device information. This script automatically initializes the FES-device with the given parameters of the configuration file and open a default model which includes the level 2 Matlab S-function block called FES_block. It is possible to change the amplitude regulation mode to manual if it isn't intended to use the configured values but changing the values within a Simulink Dashboard during stimulation. Anyway, a configuration file must exist!

The default FES - model includes the FES-communication block as well as 2 control methods, the control via a shoulder position sensor and via Keyboard. For detailed description of how to use the FES-block see chapter 2.3 and chapter 2.4 in the according thesis or see explanation within the Matlab script "sFES_block.m".